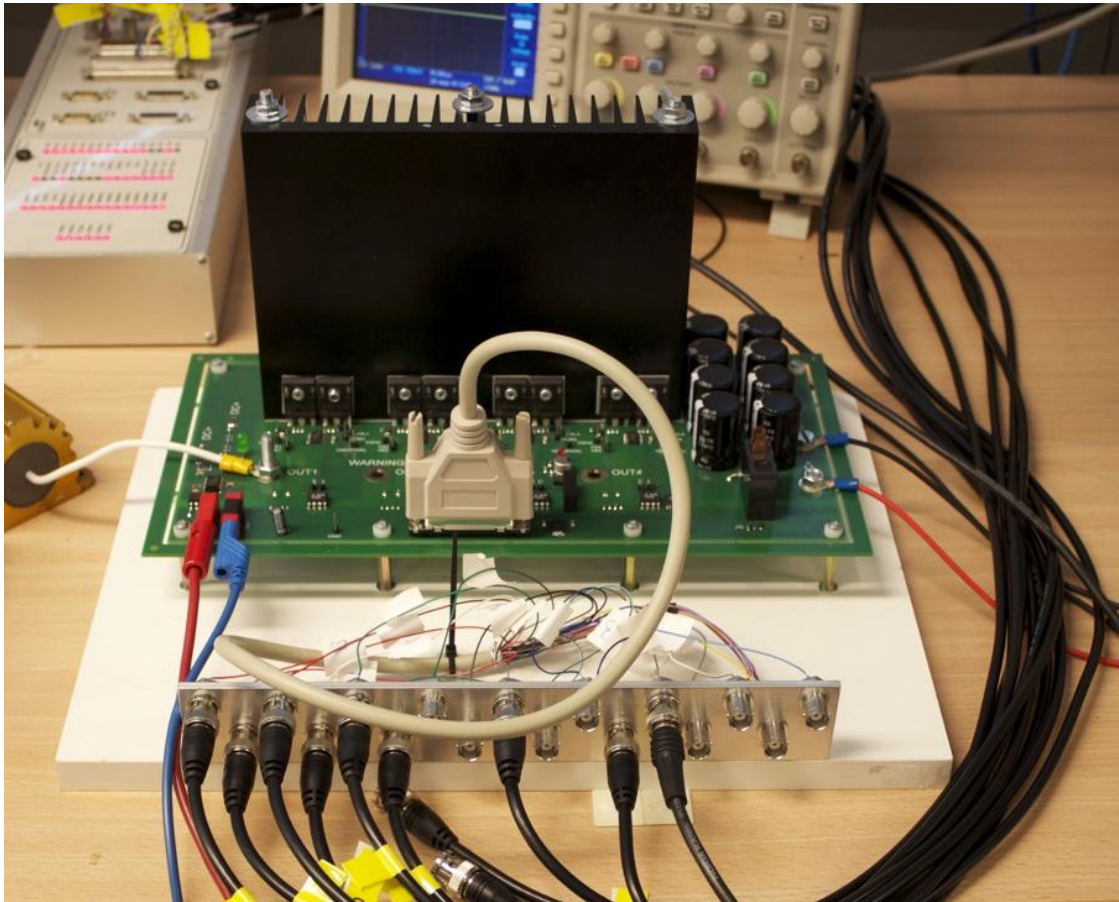# CHALMERS

Four Phase Switch-Mode Inverter
Construction and Evaluation
Master of Science Thesis

KRISTOFFER BERNTSSON

Department of Energy and Environment
Division of Electric Power Engineering
CHALMERS UNIVERSITY OF TECHNOLOGY
Göteborg, Sweden, 2010

Abstract

In this project a four phase switch-mode DC/AC inverter was designed, built and evaluated. From Etteplantech and Chalmers University of Technology a common need for a well behaving and versatile inverter in the medium power range was found. The final product was targeted to be able to deliver up to 7 kW of power, with an input DC voltage of 600 V.

The finished product managed to operate a 4 kW induction machine to its limits, with a maximum tested switching frequency of 18 kHz. This must be seen as a success. A larger strain on the inverter was not done due to lack of a larger machine, but individually the 600 V supply voltage and the 10 A per phase output current was tested successfully.

The resulting inverter is very versatile; with the right control system it's capable of operating any electrical machine. The input control logic can handle both 3.3 and 5 V signals, while the input DC voltage can be in the 25 to 600 V range.

Basic simulations done during the project shows that an RC-snubber would be able to lower the EMI by lowering the *dv/dt* during switching, while introducing extra losses in the snubber circuit without lowering the losses in the IGBTs, only moving them from turn-off to turn-on. In the finished hardware, the snubber circuit was therefore only prepared for, not implemented.

ii

Acknowledgements

Contents

1   Introduction

1.1   Purpose

The aim of the project is to design, build and evaluate a four phase switch-mode inverter in the medium power range, suitable as an electric motor drive. Behind the development of the project is a desire from the two partners, Etteplantech and Chalmers University of Technology, to have a well behaving and versatile inverter that can be used as a basis for future developments in the electric machine drive.

The product is designed to convert power from a DC source in order to drive an electric machine in a laboratory or test setup. As such it's important for the product to be easily connectable to different power supplies and machines. Moreover, it's desirable for the product to be easily accessible and that parts are replaceable or even exchangeable.

The product is not a fully operational motor drive. It will not have a built in controller of any kind, but shall easily be connected to a separate one, either a microprocessor or a dSPACE system.

As a test platform it's intended to be used by people with skills in electrical engineering. Further it's supposed to be an open test bed, without an enclosure.

1.2   Terminology and Definitions

PCB	Printed Circuit board	(no components)
PBA	Printed Board Assembly	(PCB with components)
TBD	To Be Defined	
TBP	To Be Proposed	
DC	Direct Current	
AC	Alternating Current	
PMSM	Permanent Magnet Synchronous Machine	
LVD	Low Voltage Directive	
MOSFET	Metal-Oxide-Semiconductor Field Effect Transistor. The MOSFET used in the tests is Infineon's CoolMOS transistor IPW90R120C3 (models and samples provided by Infineon)[1].	
CoolMOS	A type of MOSFET developed to have a much lower $R_{ds(on)}$ than comparable MOSFETs.	
IGBT	Insulated Gate Bipolar Transistor. The IGBT used in the simulations is Infineon's IKW15N120T2 with built in anti-parallel diode (model and samples provided by Infineon)[2].	
Gate Driver	IC used to provide the needed gate voltages and currents. The driver used in the tests is International Rectifier's Driver IC IR2214SSPbF[3].	
SiC Schottky Diode	Silicon Carbide Schottky Diode. The model used in the simulations is Infineon's SDT12S60[4].	

---

[1] (Infineon Technologies AG, 2008)
[2] (Infineon Technologies AG, 2008)
[3] (International Rectifier, 2007)
[4] (Infineon Technologies AG, 2008)

2 General three phase DC/AC inverter theory

In this section the basic theory behind a general three phase inverter is covered. All discrete parts in this theory section are assumed to be ideal.

2.1 Schematics

In Figure 2-1 an overview of the three-phase inverter is shown. Three legs, consisting of two switches and two freewheeling diodes each, makes up for the main parts of the inverter[5]. The upper transistor/diode pair is called the high side, and the lower the low side.
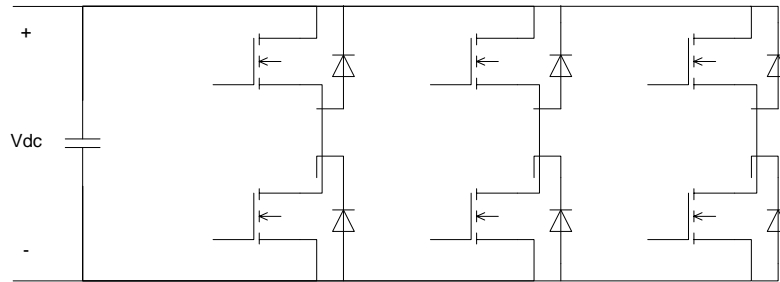
Figure 2-1 Basic schematics of a three phase inverter

When the high side switch is on, the output phase voltage equals the DC bus voltage, while the output phase voltage is zero with respect to the negative DC bus voltage when the low side switch is turned on. By switching the six switches in a controlled manner, almost any voltage waveform can be achieved. The most common control scheme when driving an electric machine is the pulse-width-modulated (PWM) scheme, covered below.

2.2 PWM

The foundation of the PWM technique is the modulation of the pulse width, accomplished with the help of a triangular wave. The triangular wave, which frequency sets the switching frequency, f_s, of the inverter, is compared with another waveform, the control waveform. The control waveform modulates the duty-ratio of one inverter leg and has the so-called fundamental frequency f_1. The output from the inverter is not perfectly comparable to the control waveform, since the output is either the full DC voltage or zero voltage. The ratio between the switching frequency and the fundamental frequency is called the frequency modulation ratio m_f, and is defined as

$$m_f = \frac{f_s}{f_1}$$

<div align="right">*2-1*</div>

The amplitude modulation ratio m_a is defined as

$$m_a = \frac{\hat{v}_{control}}{\hat{v}_{tri}}$$

<div align="right">*2-2*</div>

where $\hat{v}_{control}$ is the control signal peak amplitude and $\hat{v}_{tri}$ is the triangular wave peak amplitude, which is generally kept constant.

A good design consideration is to let m_f be an integer with a multiple of 3. This will eliminate the even harmonics as well as the most dominant harmonics in the line-to-line voltage.

---

[5] (Mohan, Undeland, & Robbins, 2003)

Normally m_a is kept at less than or equal to 1, where the output voltage varies linearly with the amplitude modulation ratio. The peak value of the output voltage in one leg is then

$$(\hat{V}_{AN})_1 = m_a \frac{V_d}{2}$$

<div align="right">2-3</div>

With a sinusoidal output voltage, the line-to-line rms value of the output can be written as

$$V_{LL_1} = \frac{\sqrt{3}}{2\sqrt{2}} m_a V_d$$

<div align="right">2-4</div>

If the amplitude modulation ratio exceeds 1, the overmodulation region is entered, where the amplitude of the output voltage no longer increase proportionally with m_a, causing greater difficulties to control the inverter. The maximum output voltage that can be reached is

$$V_{LL_1} = \frac{\sqrt{6}}{\pi} V_d$$

<div align="right">2-5</div>

when the inverter enters the square-wave mode of operation at m_a = 3.24, for a sinusoidal $v_{control}$.

2.3 Harmonics

Due to the design of the inverter, where it outputs full voltage or zero voltage, the output curve will have harmonics at multiples of m_f, the higher the value, the higher frequency of the harmonics. High frequency harmonics are more suppressed by an inductive load, while low frequency harmonics will cause greater losses in an electric machine. The important consideration that has to be made is the one between higher losses in the inverter or higher losses in the machine.

2.4 Electric machines and motor drive basics

The PWM switched inverter described above provides the foundation to drive a wide range of electric machines; induction machines, brushless DC-machines and permanent magnet synchronous machines.

Different control techniques are needed for different types of motors, for example an induction machine works best with a sinusoidal voltage and current curve, while a BLDC-machine wants a square waved current, achieved by either a sine wave voltage curve or a trapezoidal curve.

2.5 Power transistors

2.5.1 Metal-Oxide-Semiconductor Field Effect Transistor (MOSFET)

MOSFETs are popular because of their fast switching speeds in the range of a few tens of nanoseconds to a few hundred nanoseconds depending on the device type. Because of the fast switching speeds they can have low switching losses and therefore higher switching frequencies can be used. For a PWM controlled motor drive, a higher switching frequency is desired because of the harmonic components in the output signal as discussed in Section 2.3 above. When you push the harmonics to a higher frequency, they will be suppressed more by the motor that acts as an inductive load. If a filter is to be implemented it can be made with smaller component values since it's easier to filter out higher frequency components.
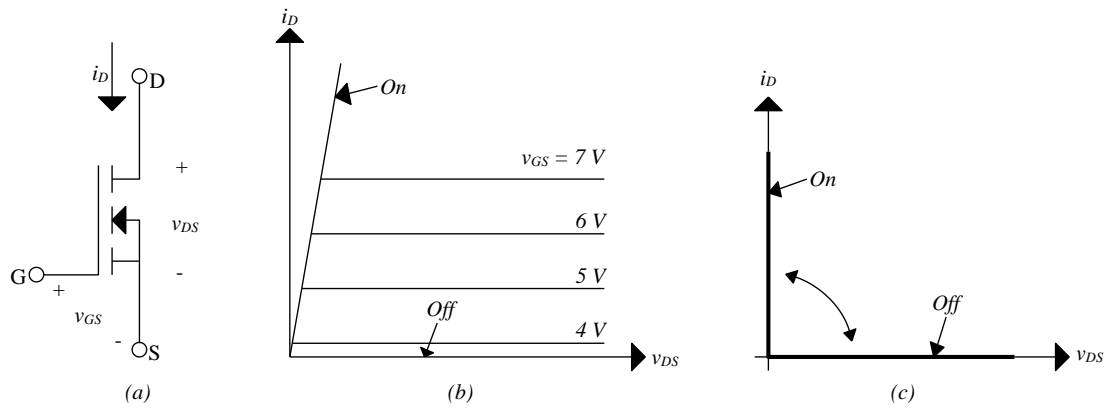
Figure 2-2 An N-channel MOSFET: (a) symbol, (b) i-v characteristics, (c) idealized characteristics

The N-channel MOSFET is controlled by applying a voltage over the gate and source. When v_{gs} is zero, the switch is closed and in the on-state it has two operating modes; the ohmic region and the saturated region, depending on the voltage level. In the ohmic region the switch act as a resistor and the voltage drop can be calculated with ohm's law. The resistance is called $R_{DS(on)}$. If v_{gs} isn't high enough for a given current, se Figure 2-2b, the MOSFET works in the saturated region. It needs a continuous voltage source to conduct, but only needs a gate current during the switching action when the gate capacitance is being charged or discharged.

The MOSFET's biggest weakness lies in the high power area. When the voltage blocking capability of the transistor is increased, $R_{DS(on)}$ also increases. The high on-resistance causes a high energy loss when a large current flows through it, according to

$$P_{conduction} = R_{DS(on)}I_{DS}^2$$

2-6

where I_{DS} is the drain current.

A modified design called CoolMOS™ has been developed to reduce this problem. It can reduce the on-resistance by a factor of 5. Naturally there are a lot of different products on the market and the specifications vary. An example is Infineon's IPW90R120C3[6], whose most important data can be viewed in Table 2-1.

Table 2-1 A selection of data from the datasheet of IPW90R120C3

Data of MOSFET: IPW90R120C3			
V_{DS} @ T_J = 25 °C		900	V
$R_{DS(on),max}$ @ T_J = 25 °C		0.12	Ω
Continuous drain current	T_C = 25 °C	36	A
	T_C = 100 °C	23	A
Package		PG-TO247	

2.5.2 Gate-Turn-Off Thyristors (GTO)

A GTO can block voltages up to 4.5 kV and handle currents up to a few kA (Mohan, Undeland, & Robbins, 2003). However, GTOs are too slow for this product (switching times between a few μs to 25μs) and extremely high voltage blocking capabilities are not needed for this product.

---

[6] (Infineon Technologies AG, 2008)

2.5.3 Insulated Gate Bipolar Transistor (IGBT)

According to (Mohan, Undeland, & Robbins, 2003) the "IGBTs have some of the advantages of the MOSFET, the BJT, and the GTO combined. Similar to the MOSFET, the IGBT has a high impedance gate, which requires only a small amount of energy to switch the device. Like the BJT, the IGBT has a small on-state voltage even in devices with large blocking voltage ratings (for example, V_{ON} is 2-3 V in a 1000-V device). Similar to the GTO, IGBTs can be designed to block negative voltages, as their idealized switch characteristics is shown in Fig. 2.12c (Note: the figure is named Figure 2-4 in this document) indicate".

The IGBT is controlled in the same manner as the MOSFET and the same driver can be used for the two devices. During turn-on the IGBT acts like a MOSFET, with the same switching speed. The turn-off process is different; the first part is similar to the MOSFET when V_{CE} rises to the blocking voltage and i_C then falls rapidly. But as seen in Figure 2-3 the current fall is divided into two parts, the MOSFET part and the BJT part (usually called the "tail"). This latter part is much longer than the first, giving IGBTs slower turn-off and higher switching losses compared to MOSFETs. Due to the nature of the IGBT, a trade-off between on-state losses and faster turn-off times must be made by the manufacturers. Tricks are used, to some extent, to get around the problem, either by using a punch-through design, or by design the device so that the MOSFET part of the turn-off is as large as possible (the timing is the same, but the losses are lower due to the lower current magnitude of the tail).

A selection of data of a commercially available IGBT is shown in Table 2-2.
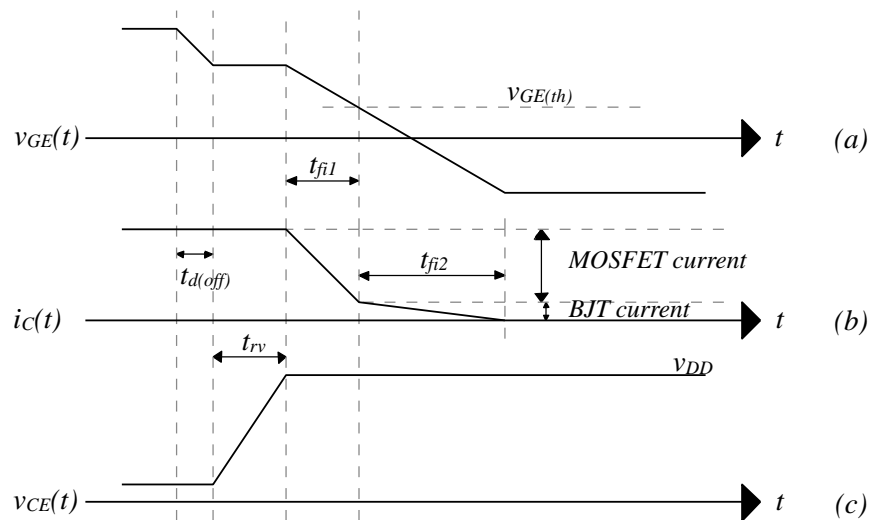
Figure 2-3 IGBT turn-off waveforms for an embedded step down converter

The strengths of the IGBT is its high blocking voltage and high current capability, up to 1700 V and several hundred amperes.

Conduction losses in an IGBT can be calculated by the following equation

$$P_{conduction} = V_{CE(sat)}I_C$$

(a)

(b)

(c)
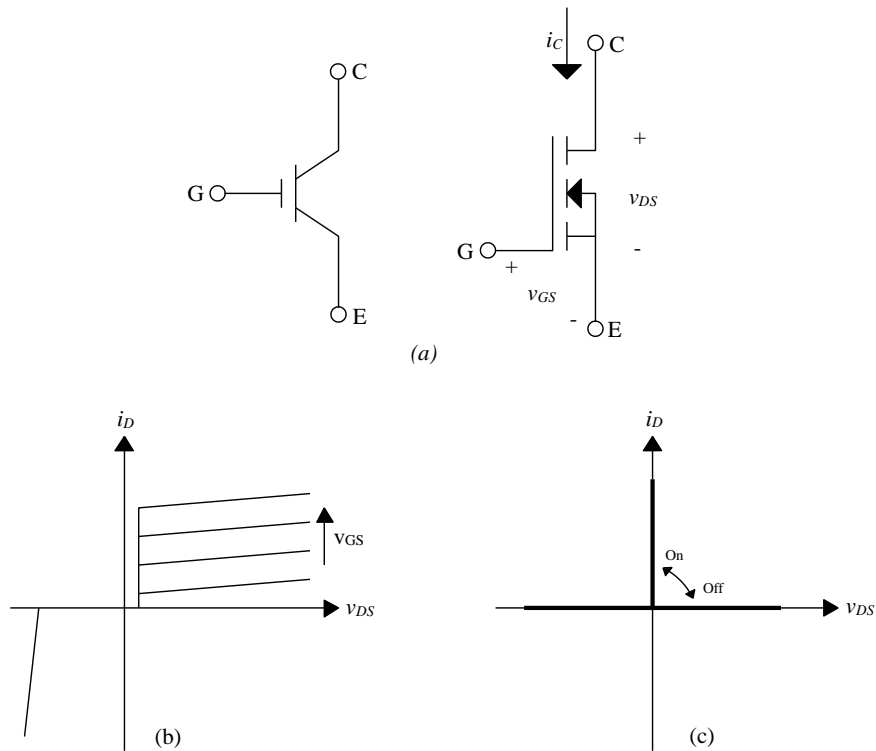
Figure 2-4 An IGBT: (a) symbol, (b) i-v characteristics, (c) idealized characteristics

Table 2-2 A selection of data from the datasheet of the IKW15N120T2

Data of IGBT: IKW15N120T2			
V_{CE} @ T_J = 25 °C		1200	V
$V_{CE(sat)}$ @ T_J = 25 °C		1.7	V
Continuous collector current	T_C = 25 °C	30	A
	T_C = 110 °C	15	A
Total switching energy @ T_J = 25 °C, I_C = 15 A		2.05	mJ
Package		PG-TO247-3	

3 The hardware

3.1 Overview

The project aim is to produce a PWM switched four phase DC/AC inverter. A functional overview is shown in Figure 3-1, where the different building blocks are shown. Below they will be discussed in detail.
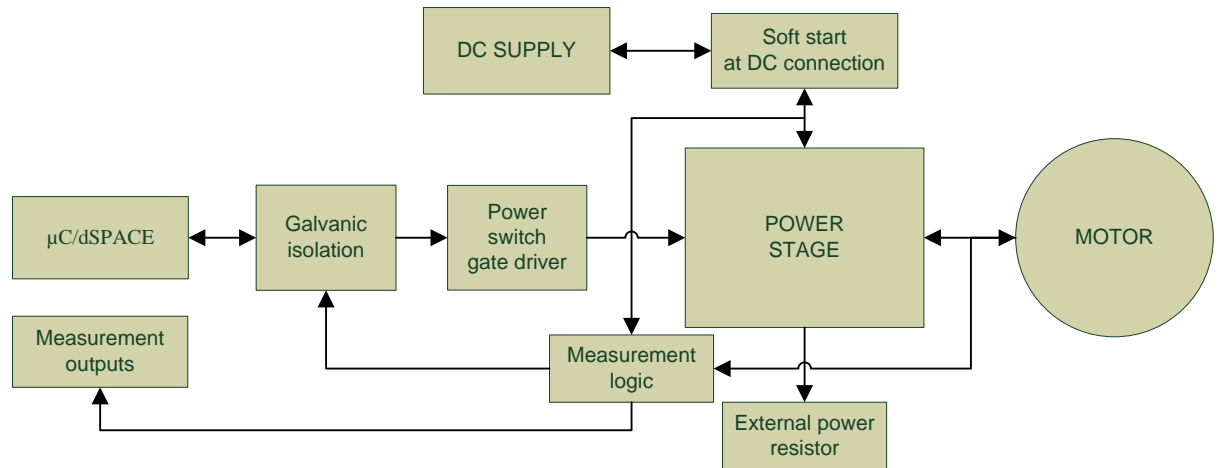
Figure 3-1 Functional overview of the converter

3.2 Requirement specification

3.2.1 General

This requirement specification was worked out in cooperation between Etteplantech and Chalmers. Since it's not a product designed for the market, some requirements normally seen is here not applicable.

3.2.2 Product perspective

The product is to be used in a test setup or in a laboratory.

3.2.3 Typical users

The product is designed to be used by individuals with skills in electrical power engineering and electrical safety regulations.

3.2.4 Market requirements

Since the intended use for the product is a test setup, no special requirements from the market is considered. A possible update on the product designed for the market could be realized in a later stage.
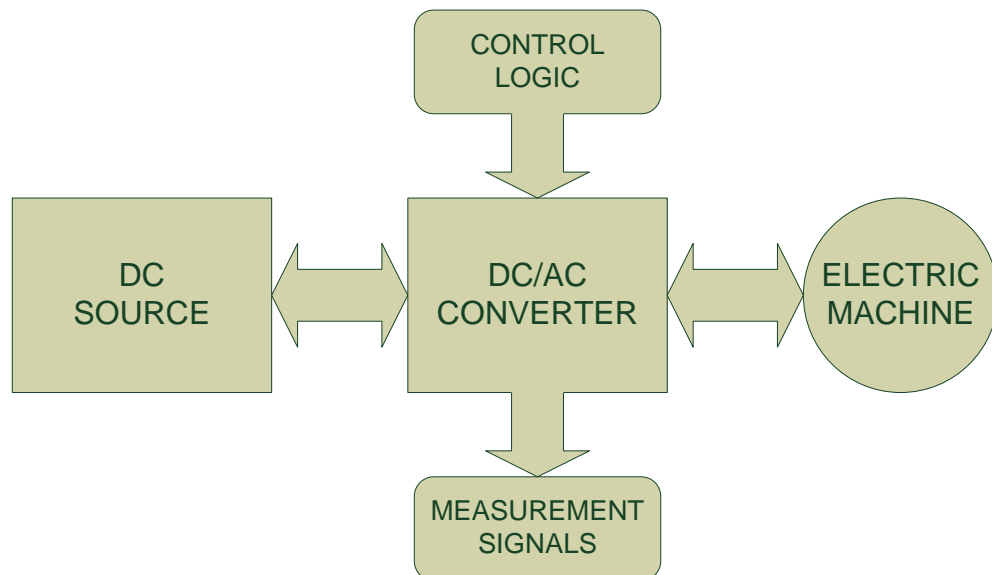
Figure 3-2 Functional overview of the product

3.2.5 Functional requirements

- Convert power from a DC source to an AC load
- Drive a general balanced three phase load (for instance a PMSM)
- Be able to brake a general balanced three phase machine
- Ability to be controlled by either a microcontroller (e.g. Cortex M3) or a dSPACE system
- Be able to measure current in all phases
- Be able to measure voltage on the supply side
- Possibility to exchange the power electronic components through re-soldering
- Provide 4 output phases
- General connections to supply and load for easy connection to different sources and machines, see Section 3.2.7 for specifications
- Passively air cooled
- Separated voltage level for logic signals, galvanicly isolated
- Safety blanking times in hardware

Functional wish list

- Be able to measure the temperature of the power electronic components
- Automatic overvoltage protection
- Possibility to remove the hardware blanking times

3.2.6 Man-machine requirements

The product is intended for a laboratory setup and hence only qualified users are working with the product. Further it's not intended for the market. Therefore the requirements on "looks" are limited. Instead it's important that components and measurement points are easily accessible to the user.

3.2.7 Interface requirements

- Galvanicly separated low voltage and high voltage side, with logic and power circuitry respectively
- Exchangeable power electronic components through re-soldering

- Connections to a microprocessor or a dSPACE system. The two different controllers should be switchable. The controller signals should work with CMOS signals
- The DC source should be connected through M6 screws
- The load should be connected through M6 screws
- Galvanic isolation between logic and drive and measurement circuits
- Possibility to add capacitances parallel to power switches
- Possibility to add an RC snubber over each power switch
- Control logic and drive circuit power supply are separated from the main DC supply

For connection to the dSPACE system:
- 17 BNC connections (5V logic)

3.2.8 Performance requirements

- Handle input voltages between 0 and 600 V_{DC}
- Provide up to 10 A_{rms} per phase of output current
- Switching frequencies up to 20 kHz
- Handle maximum currents of up to 15 A per phase
- Target: 7 kW of output power (note that when driving an inductive electric machine that draws a lot of reactive power, the output current to be about 25 % higher for the same active power)
- Measure phase currents with an accuracy of 1 % and a bandwidth of 50 kHz
- Measure input DC voltage with resistive voltage divider, using jumpers to change divide ratio for different DC inputs. A linear optocoupler to transfer the downscaled voltage to the low voltage side
- Soft start at DC connection
- Large input capacitance to hold a steady DC voltage. It should be able to maintain the voltage level above 80% for 2 ms in the event of a loss of the DC source
- Powerful drive circuits to make fast switching possible

3.2.9 Rules and regulations

Wish list:
- Comply with the LVD
- Comply with the RoHS directive
- ISO6469-3

3.2.10 Component and material requirements

- The product must not include any of the banned substances in the RoHS directive
- The power transistors should be exchangeable, therefore a standard case style such as TO220/247 should be used

3.2.11 Mechanical requirements

The PCB should be mounted on a stand or plate that serves as a foundation for the product, so that it can be placed on different surfaces. The foundation should also provide the BNC connectors for the dSPACE system to relieve the PCB for the physical strain when connecting and disconnecting the cables. A further requirement on the ground plate is that it should provide a layer of electrical isolation between the PCB and the surface it's placed on.

3.2.12 Cost requirements

The prototype nature of the product leads to a performance over cost thinking.

3.2.13 Size requirements

Because of the prototype stage of the product the size requirements are loose.

3.2.14 Reliability requirements

The product should be able to handle the testing and laboratory environment for which it is intended.

3.2.15 Testability requirements

- Measurement points should be available as pins on the board

3.2.16 Environmental requirements

3.2.16.1 Electrical environment

- As good EMI performance as possible with a standard inverter design

3.2.16.2 Climate environment

- The product should be able to work in the temperature range between 10 and 50 °C, in an environment where the air is standing still

3.2.17 Availability requirements

The prototype nature of the product limits the availability to a single unit.

3.2.18 Safety requirements

3.2.18.1 Safety standards

- Comply with the LVD

Wish list:

- Follow the highest insulation classification according to the ISO6469-3 standard (Class II: Double or reinforced insulation a.c.).

3.2.18.2 Safety devices

- A light to signal that the device is on

Wish list:

- Overvoltage protection. In the case that energy flows to the DC source and that source doesn't have the capability to absorb the energy, a device burning the excess energy through a load resistor is to be implemented. The resistor has to be supplied externally.

3.2.18.3 Marking

- Marked with logo and warnings

3.2.19 Production requirements

- Manual assembly required

3.2.20 Start of operation requirements

- Soft start when connected to DC source

3.2.21 Maintenance requirements

The product is to be used in an open test bed; hence it shouldn't be put under a lot of physical stress. If the temperatures stay within the specified limits the only maintenance required is to keep the components free from dust.

3.2.22 Educational requirements

- Operating instructions should be, describing the functions, uses and limitations of the product

3.2.23 Equipment needed to use the product

- DC voltage supply, one for power plus one for the drive circuit (15 V)
- Balanced one, two, three or four phase inductive or resistive load
- Control logic (3.3 or 5 V)

3.3 DC supply circuitry

3.3.1 Capacitor

The input capacitor has the task of keeping the supply voltage stable to ease the control of the power transistors. According to the requirement specification the input capacitor should be able to hold the voltage above 80 % during 2 ms if the supply voltage is lost. Considering the case with a motor load, the current is assumed to be constant during the 2 ms. At a maximum load of 7 kW and 600 V input voltage, the DC load current is 11.7 A. The total charge taken from the capacitor is then

$$Q = It = 11.7A \times 2ms = 23.4mC$$

<div align="right">3-1</div>

The charge left in the capacitor after 2 ms should be 80 %, then the charge taken from the capacitor is 20 %. The charge stored in the capacitor is

$$Q = CV$$

<div align="right">*3-2*</div>

With V = 20 % of 600 V and Q = 23.4 mC, the capacitance equals 195 µF.

The worst case ripple current going through the capacitor is a square wave signal with an amplitude of 10 A at a frequency equal to the switching frequency of the system. The actual ripple current during normal operation of the converter (three phase motor drive) will be less due to the nature of the three phase system where always two legs are conducting in opposite direction and hence cancel each other out seen from the supply.

To handle the voltage and ripple current requirement a bank of eight 100 µF, 400 V capacitors were chosen, two in series and four legs in parallel. Each can handle ripple current of 1.3 A at 10 kHz and 105 °C. The worst case 2.5 A per leg can be handled by the capacitors at the much lower anticipated temperature of 25 °C. Also a shorter life span is acceptable in this project.

To keep each capacitor within its voltage limits a voltage divider was implemented; two 1 MΩ resistors in parallel with the capacitors, see Figure 3-3. To make sure that the current is spread out evenly over the bank, the negative side is connected in one point on the PCB.
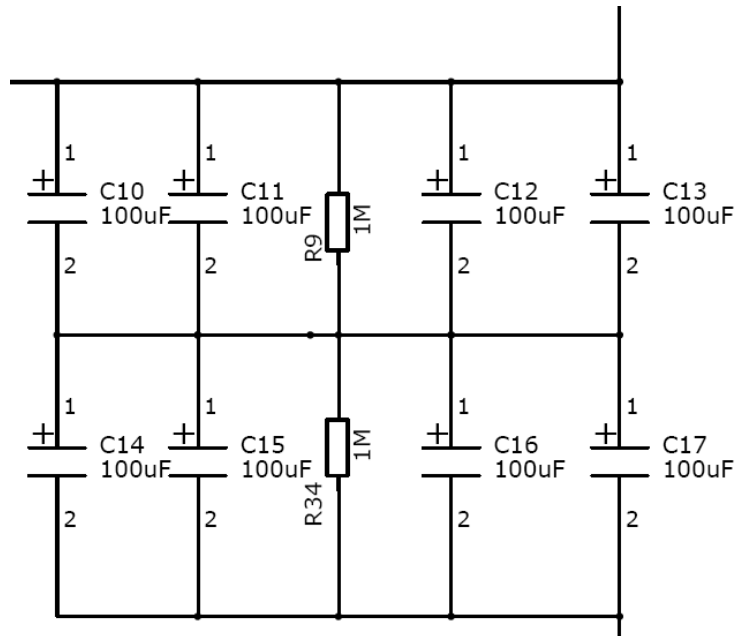
Figure 3-3. DC supply capacitor bank setup.

The capacitor choice: 8 x 100 μF, 400 V, Panasonic EETED2G101BA

Voltage divider: 2 x 1 MΩ, from stock (SMD, 1206)

3.3.2 Soft starter

To prevent large surge currents when the DC source is connected to the large DC side capacitor, a soft starter is implemented. The soft starter is shown in Figure 3-4. When the supply is connected to the terminals, a resistor is connected in series with the capacitor. A relay controlled by the control logic connects the capacitor directly to the DC supply terminals when V_{in} has reached the voltage level of the DC source. The soft starter resistor should be large enough to prevent current spikes and small enough to charge the capacitor within a reasonable timeframe. The time constant of the RC-circuit present when connecting the DC source is calculated by

$$\tau = RC$$

3-3

A time constant of 1 second is suitable for this project. With a capacitor of approximately 200 μF, a resistance of 5 kΩ is needed. The maximum current flowing through the resistor is calculated as follows

$$i_{max} = \frac{V_{DC,max}}{R_{soft}} = \frac{600V}{5k\Omega} = 120mA$$

3-4

and the maximum power dissipated in the resistor can be found as

$$P_{R,max} = \frac{V_{DC,max}^2}{R_{soft}} = \frac{600V^2}{5k\Omega} = 72W$$

3-5

These numbers are easily managed by a power resistor since the duration of the power spike is less than a second (the time constant τ is 1 second).

Choice of relay: Panasonic ALE1PB12; 16 A, 12 V

Choice of soft starter resistor: 4.7 kΩ

Figure 3-4 Schematics of the soft starter

3.3.3 Protection

To make sure that the capacitors in the circuit are discharged, a discharge resistor is connected in parallel to the input capacitor. Since it's always connected it will always be conducting current, introducing a constant loss of power.

The discharge current is used to drive an indicator LED connected in series with the resistor to alert the user that the system is 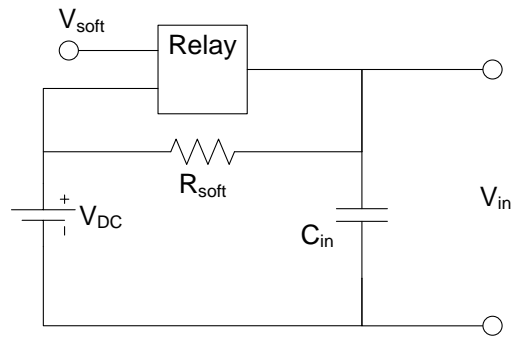energized. A LED with a forward voltage of 1.9 V and an average current of 2 mA is used. With a maximum voltage of 600 V the resistor should be 300 kΩ to limit the current to 2 mA. The time constant of the resulting RC-circuit is 60 seconds, and the average power loss at 600 V is 1.2 W.

Since the product is to be able to work with a wide range of input voltages, a simple setup with 4 series connected resistors were chosen, to safely scale down the voltage. The four base levels are 600 V, 300 V, 100 V and 25 V. Around these levels the LED will glow close to its optimum and the capacitors will discharge in a timely manner.

LED choice: Vishay TLLG5400; 5 mm, 2 mA

Discharge/LED resistor choice: 4 x 75 kΩ, 1 W; 2 x 75 kΩ, 1 W; 51 kΩ, 1 W; 12 kΩ, 1 W

3.3.4 Separate low voltage supply

Separate input connectors to supply the drive circuits are implemented. This solution was made to facilitate a broad DC voltage working range. Since the product is to be used in a test setup, a separate voltage source should be available. A voltage of approximately 15 V is needed to drive the low voltage circuits.

To supply the drive circuit, an isolated DC/DC converter is used with an output of 15 V. This ensures that the low voltage supply isn't stressed with a large voltage offset with respect to ground. The low voltage supply is also connected directly to the current measurement module whose output is relative to ground. A total of 67 mA can be taken from the converter. Each gate driver can an estimated current of 3.6 mA, giving a total of 14.4 mA, see Section 3.6.2.3 below for details. This current can easily be handled by the converter.

A second isolated DC/DC converter is used to provide +/- 5 V to the high voltage side of the converter, driving five optocouplers and one OP-amp. A total of 100 mA can be taken from each leg of the converter. The optocouplers take a total of 25 mA and the OP-amp about 12 mA, 6 mA on each leg, maxing out at around 30 mA, well within the converter's limits.

To provide 5 V to the low voltage side of the optocouplers, a non-isolating voltage regulator was chosen. The unit can deliver a maximum of 1 A, well above the needs of the system.

Isolated DC/DC converter choice: Murata NMV1515, 15 V, 1 W, 1 kV$_{DC}$ isolation; Murata NMA1505, +/- 5 V, 1 W, 1 kV$_{DC}$ isolation

Non-isolated voltage regulator choice: On Semiconductor MC7805CDTG, 5 V, 1 A

3.4   Logic interface

3.4.1   Interface

The interface should be able to handle two separate control systems, both a microprocessor and a dSPACE system. They should not be connected simultaneously.

The microprocessor PBA should be connected with a 25-pole D-SUB.

The dSPACE system will be connected through 17 BNC connectors, mounted on the base plate for improved ruggedness. On the base plate wires connect the BNC connectors with a 25 pole D-SUB connector that can be easily connected to the Power PBA. The D-SUB can be seen in Figure 3-5 and the BNC panel in Figure 3-6, while its connections can be viewed in Table 3-1.

By using the same connector for both control options it's impossible to connect both the microprocessor and the dSPACE system simultaneously.
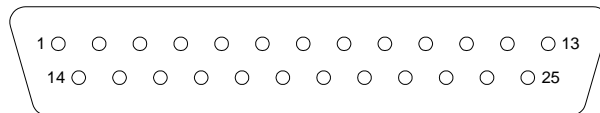
Figure 3-5 The 25-pin D-SUB connector seen from above
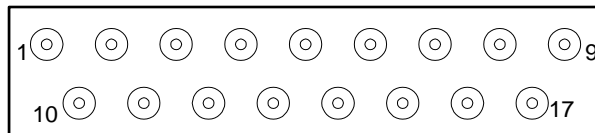
Figure 3-6 The BNC panel

3.4.2   Voltage level

The logic signals to the drive circuits works at a voltage level of 3.3 or 5 V.

3.4.3   Ground plane

Two ground planes are implemented on the PCB, one for the high voltage side and one for the low voltage side. The two has galvanic isolation between them; the isolation is further presented in Section 3.4.4 below.

3.4.4   Galvanic isolation

To facilitate easy connections and protection to the control circuit, the control signals are galvanicly isolated with optocouplers. This ensures that the control circuit and drive circuit is electrically separated and can use separate ground planes and power supply (the isolated power supplies are presented in section 3.3.4 above). To further enhance the separation the PCB is divided into two areas, a high voltage side and a low voltage side, creating two clearly defined zones.

Table 3-1 Connection scheme for the D-SUB and BNC connectors

25-pin D-SUB		BNC panel	
1	Relay	1	1H
2	Fault	2	2H
3	SD	3	3H
4	FLT_CLR	4	4H
5	4L	5	FLT_CLR
6	4H	6	Fault
7	3L	7	I1
8	3H	8	I3
9	I3	9	V_{dc}
10	2L	10	1L
11	2H	11	2L
12	1L	12	3L
13	1H	13	4L
14	GND	14	SD
15	GND	15	Relay
16	GND	16	I2
17	GND	17	I4
18	GND		
19	GND		
20	I4		
21	GND		
22	I2		
23	I1		
24	Vin		
25	GND		

Transmission of the logic signals over the barrier is made by optocouplers. The chosen ones are called digital isolators and can work at frequencies up to 50 MHz and can be driven directly from the microprocessor, since a very low current of only 10 μA is needed to change the state of the digital isolator. It's also compatible with both 3.3 V and 5 V systems. The optocoupler needs 5 V on both sides of the isolation barrier in order to work and they typically consume 0.018 mA on the low voltage side and 5 mA on the high voltage side. Each optocoupler can transmit two signals and one unit is used for each gate driver, resulting in four units. A fifth unit, capable of transmitting two signals in each direction, is used to send and receive fault signals to the gate drive system. This unit needs 5 mA on both sides of the voltage barrier.

On both sides of the optocouplers a 47 nF ceramic capacitor is used to decouple the units as recommended by the data sheet of the optocouplers.

Measuring the main DC voltage and transmitting the signal across the voltage barrier is a system of one OP-amp and one linear optocoupler, seen in Figure 3-7. The voltage is first scaled down to approximately 3 V with a voltage divider. Four different resistor setups are used to provide the voltage divider (R1); 6.2 MΩ, 3 MΩ, 1 MΩ and 220 kΩ for 600 V, 300 V, 100 V and 25 V working voltages respectively. "This voltage is offset by the voltage level of the photocurrent flowing through R3. This photocurrent is developed by the optical flux created by current flowing through the LED. Thus as the scaled monitor voltage (V_a) varies it will cause a change in the LED current necessary to satisfy the differential voltage needed across R3 at the inverting input."[7] The output is targeted to be 2.5 V when the input voltage is at the chosen working voltage (600 V, 300 V, 100 V or 25 V). The circuit needs to be calibrated to get an accurate function of the voltage since every optocoupler is unique. The resulting function will follow these lines

$$V_{DC} = \frac{(R_1 + R_2)(V_{out} - V_{base})}{kR_2}$$

3-6

where *k* is a constant designed to be close to 1 and V_{base} is an offset close to zero.
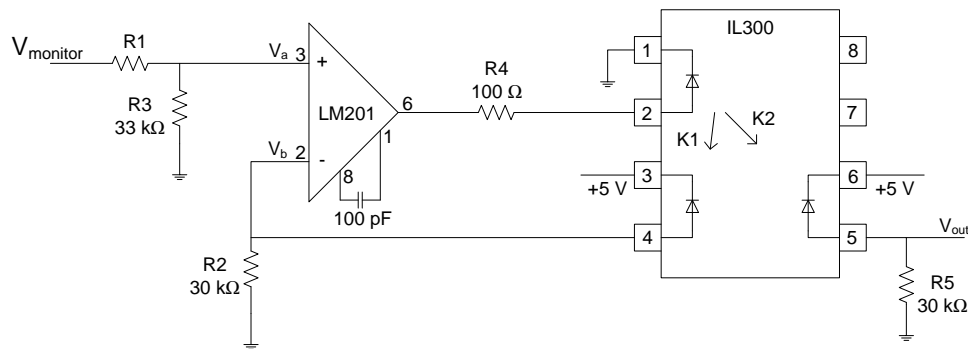
Figure 3-7 Voltage measurement circuit

Choice of optocoupler: Avago HCPL-9030; Avago HCPL-901J
Choice of linear optocoupler: Vishay IL300
Choice of OP-amp: ST LM201AN

3.4.4.1 Results from the verification of the hardware

Unfortunately a mistake was made in the design that was only discovered after the assembly of the inverter; the fault signal level on the high voltage side has a default non-fault level of 15 V. Since the optocouplers has a built in voltage regulator, it holds the voltage at a maximum of 5 V, constantly putting the drive circuit into its fault state. To solve the problem, the two legs off the optocoupler connected to the drive circuit were soldered off, hence not connected. The result: **no fault signals can be sent to, or from, the controller. The only fault indication is the red LED on the PBA.**

3.4.5 Protection against simultaneous turn on of both high-side and low-side switch

The chosen gate driver IC has a minimum built in blanking time of 330 ns, see Section 3.6 for details.

---

[7] (Vishay Semiconductors, 2005)

3.5   Power Transistor

3.5.1   MOSFET and IGBT comparison

Given the above discussion about the different transistor options, the choice stands between the MOSFET and the IGBT. Both switches are controlled by the applied gate voltage, and they can both manage the required switching frequencies for the product at hand. The choice will therefore mainly come down to price and energy losses produced in the device. There are two main components to consider when calculating the power loss in the device; switching losses and conduction losses.

In Figure 3-8 the switching characteristics of a simplified clamped-inductive-switching circuit is shown. During the switching action both the voltage and current is on, and the switching losses can be calculated as follows

$$P_{switch} = \frac{1}{2} V_d I_0 f_s \left(t_{c(on)} + t_{c(off)} \right)$$

3-7

where V_d is the applied voltage, I_0 is the current, f_s is the switching frequency and $t_{c(on)}$ and $t_{c(off)}$ is the turn-on and turn-off switching times respectively[8]. Unfortunately the manufacturers don't provide enough information; especially the current tail time of the IGBT is usually missing. Important to note here is that the $t_{c(on)}$ and $t_{c(off)}$ depend on the design of the circuit where the voltage rise and fall times are decided by the surrounding design while the current rise and fall times depend on the gate drivers ability to provide current. The timings given in data sheets are the minimum current rise and fall times possible by the device, measured in the 10 to 90 percent range. The total $t_{c(on)}$ and $t_{c(off)}$ will be minimum twice that figure.

Since the conduction states of the two switches differ in characteristics, two different models calculating the conduction losses have to be used. For the MOSFET the average conduction losses for a PWM controlled sine wave can be calculated with Equation 2-6, using the RMS value of the current. For the IGBTs the conduction losses can be calculated with Equation 2-7. The result is that the MOSFET's conduction losses vary with the square of the current, while the IGBT's losses vary linearly with the current. This makes it important to find components with low $R_{DS(on)}$ and $V_{CE(sat)}$ respectively.

The total power loss in the switches can be approximated by

$$P_{loss} = P_{switch} + P_{conduction}$$

3-8

because the leakage current in the off state off both transistor types is negligibly small.

In Figure 3-9 and Figure 3-10 approximate power losses in a MOSFET[9] and IGBT[10] have been calculated using the above equations at a switching frequency of 2 kHz and 20 kHz respectively. The DC voltage is held at 600 V. Note that especially the difficulty to estimate the switching times, makes an accurate switch loss calculation difficult, why only a ruff approximation is to be expected. Despite these limitations, the calculations show that the MOSFET is clearly better at lower currents and higher switching frequencies, while the IGBT is better at higher currents and lower switching frequencies. Actually the difference in switching losses should be bigger between the two because the tail current of the IGBTs are not included in these calculations, due to lack of information in the data sheet.

---

[8] (Mohan, Undeland, & Robbins, 2003)
[9] Infineon's 900 V, 0.12 Ω MOSFET; Model nr: IPW90R120C3 (Infineon Technologies AG, 2008)
[10] Infineon's 1200 V, 1.75 V IGBT; Model nr: IKW15N120T2 (Infineon Technologies AG, 2008)

During an AC motor drive operation the current flows through the diode approximately half of the time (a very rough estimation), giving rise to lower switching losses as the diode is already "turned on". The extra switching losses produced by the reverse-recovery current are not included in the calculation either, why the losses should be higher. Since these two effects are not included in the calculation, they can only be viewed as a general comparison.

Unfortunately the good performance of the CoolMOS MOSFETs cannot be utilized in the chosen invert design because of the limitations of the built in body diode. The body diode produces a very large reverse-recovery current. The large current gives rise to huge switching losses, as discovered in the simulations results below. Because the body diode starts to conduct at a low 0.7 V and because of the high voltage requirements, no discrete diode with a low enough forward voltage can be found on the market that could be used to bypass the problem.
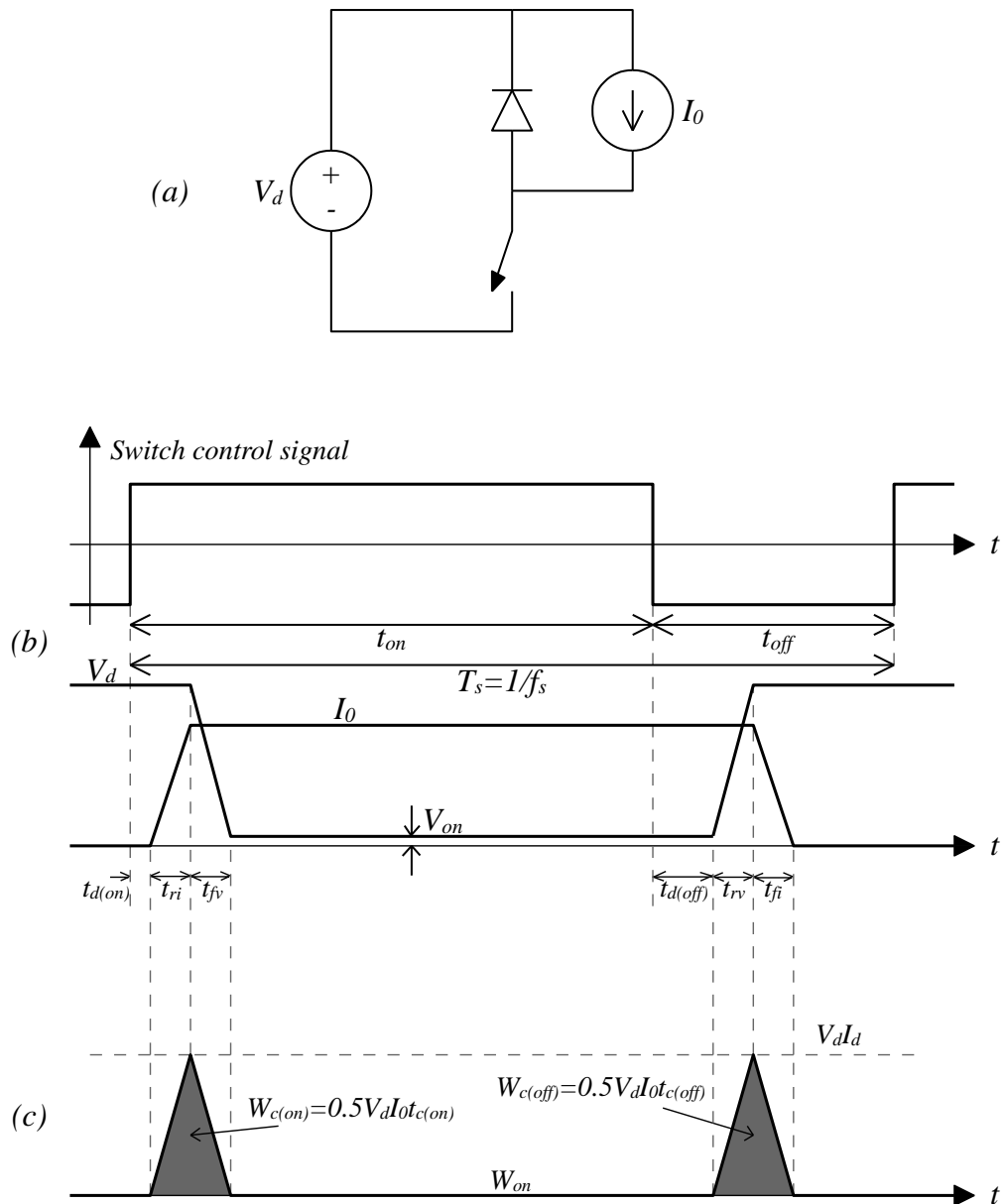

Figure 3-8 Generic-switch switching device characteristics (linearized): (a) simplified clamped-inductive-switching circuit, (b) switch waveforms, (c) instantaneous switch power loss.
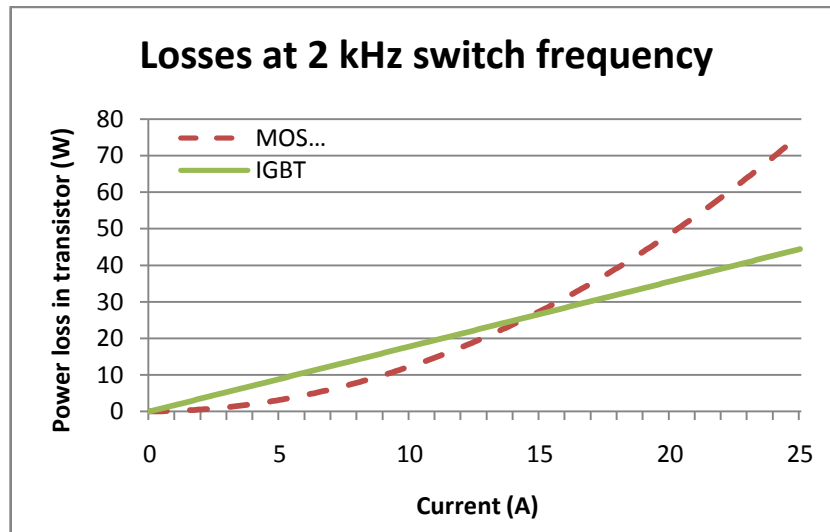
Figure 3-9 Transistor losses at different current levels when switching at 2 kHz
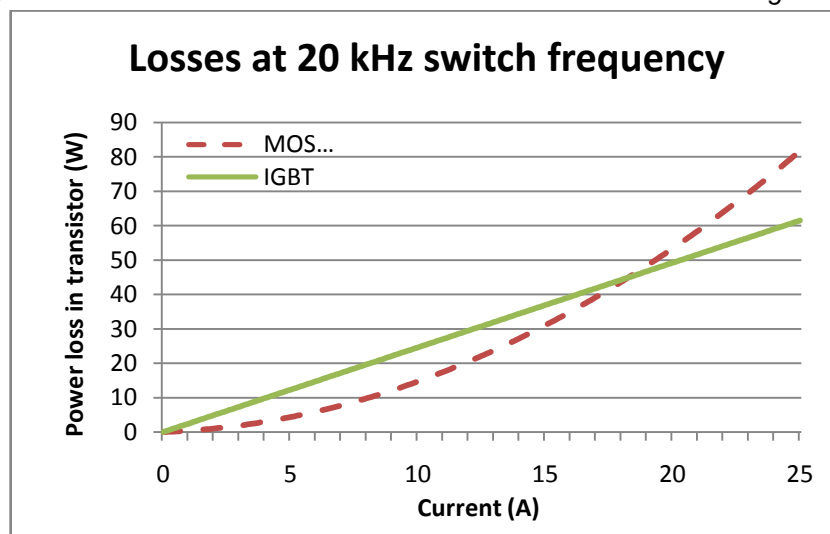
Figure 3-10 Transistor losses at different current levels when switching at 20 kHz

Chosen power transistor: Infineon IKW15N120T2, 1200 V, 15 A @ 150 °C

3.5.2 Requirements on the drive circuit

To switch the transistor the gate voltage V_{gs} should be controlled between 0 and approximately 15 V. A maximum voltage of ±20 V is tolerated by the IGBTs (IKW15N120T2). To make sure they can output the required 10 A, a minimum voltage of 10 V is needed on the gate. The drive circuit should be able to output 1 A of gate current to provide fast switching.

The switching speed of the transistors depends on the gate resistors by controlling the current flowing in and out of the gate during turn-on and turn-off. The drive circuit covered in Section 3.6 below has three different gate resistors for each gate, a turn-on, a turn-off and a soft shut down resistor.

19

3.5.3 Required cooling capability

To make an estimation of the losses in each IGBT, the specified switching energy is used as a basis for the calculation. From **Fel! Hittar inte referenskälla.** the switching energy is found at 2.05 mJ per switch. Multiplying it with 20 kHz switching frequency and then 0.5 due to the fact that half of the switches are "soft" and dividing with 1.5 since the current is 10 A compared to 15 A, the maximum switching losses amounts to **13.7 W**. The conduction losses amounts to **17 W** (10 A multiplied with 1.7 V) for a total of **30.7 W**. The total power that needs to be dissipated into the surrounding air is then **184 W** in a three phase drive setup. Table 3-2 shows the power dissipation for a few different cases. The temperature reached in the transistor junction is calculated as follows

$$T_j = P_d \left(R_{\theta jc} + R_{\theta cs} + R_{\theta sa} \right) + T_a$$

3-9

where P_d is the power that needs to be dissipated, $R_{\theta jc}$ is the thermal resistance between the junction and the casing of the transistor (or any other component), $R_{\theta cs}$ is the case to heat sink resistance, $R_{\theta sa}$ is the sink to ambient resistance and T_a is the ambient temperature. From this the needed heat sink thermal resistance can be calculated. $R_{\theta jc}$ is found in the datasheet of the transistor and for the IGBT it's 0.63 K/W. $R_{\theta cs}$ is usually a thermal transfer pad with a resistance of 0.4 K/W. To dissipate the 184 W developed in the IGBTs at full power and 20 kHz switching frequency, while keeping the junction temperature at 150 °C, the heat sink can have a maximum thermal resistance of 0.53 W/K. This figure requires either a massive heat sink (minimum 150x200 mm), or a smaller heat sink with an attached cooling fan to keep the temperature within safety margins when running at full power.

There is a possibility to use a smaller heat sink, and when needed during heavy testing connecting an external fan. The heat capability provided by the large size of the heat sink also makes it resilient to short bursts of full power operation.

Chosen heatsink: Fisher Elektronik SK47/150/SA, $R_{\theta s}$ = 0.51 K/W

Table 3-2 Total power dissipation in the 6 transistors at 600 V_{DC} and 10 A_{rms} per phase

Total power dissipation (three phase load, 10 A_{rms})		
Switching frequency	**2 kHz**	**20 kHz**
IGBT: IKW15N120T2	18.4 W	30.7 W

3.6 Drive circuit

The drive circuit amplifies the control signal from the control system and outputs a signal powerful enough to control the IGBTs by applying a voltage over the gate.

3.6.1 Available options

There are a few options when it comes to driving the gate on the IGBT. As discussed in Section 3.5.2 above, the drive circuit needs to be able to output 1 A to enable fast switching of the transistor. Because of the nature of the inverter, and the choice of an N-type transistor, the gate voltage for the high-side switch needs to be higher than the DC voltage. This issue is further discussed in Section 3.6.3 below.

The first option is to design and build a discrete driver circuit were the main parts are transistors.

The second option is to use an IC to drive the transistor gate. This makes it easier to implement, while the IC usually have extra features.

20

The third option is a drive IC for each leg of the inverter; one IC driving both the high-side and the low-side switch. This has the added benefit of fewer components and even more features, since the IC have control over the entire leg.

A forth option is a single drive IC for the entire inverter, driving six IGBTs. The benefits with this approach is even less components and ease of implementation. The drawbacks are less flexibility and difficulty to physically place all the IGBTs close to the drive circuit. Also, no single drive circuit exists to drive all eight IGBTs demanded by the requirement specification.

3.6.2 IC for each leg

With a single IC designed to drive two MOSFETs/IGBTs in a high-side/low-side setup (one half bridge), less components is needed (in this case four drive ICs). Since the high-side gate and source is floating up and down during the switching cycle, the control signals needs to be level-shifted up and down with the source voltage. The gate voltage must also be higher than the V_{DC} supply to keep the transistor open, a topic covered in Section 3.6.3 below.

The chosen driver IC is IR's IR2214SSPbF. It's capable of working with up to 1200 V and provide up to 2 A of turn-on current and 3 A of sinking current (during turn-off). Another feature is the desaturation detection that measures the voltage over the conducting transistor and compares it to a threshold voltage of 8 V (typical). If a short circuit occurs, either phase to ground or phase to phase, the large current that flows through the transistor will cause the voltage over it to increase and eventually trigger the desaturation detector (after a built in blanking time of 3 μs), which then initializes a soft shut down of the transistor and communicates the fault to the other drive ICs through the SY_FLT pin. A soft shut down is made through the soft shut down resistor instead of the regular turn-off resistor in order to limit the stresses on the rest of the system (over-voltages due to large *di/dt* plus electromagnetic emissions).

The drive IC is also equipped with three separate outputs for the gate signals to facilitate three different gate resistors, for turn-on, turn-off and soft shut down respectively. This makes it possible to more closely fine tune the switching characteristics of the transistors in order to control speed, voltage spikes and EMC.

3.6.2.1 Gate resistors

The gate resistors control the switching speed by controlling the current in and out of the gate. The resistor values were calculated from the recommendations in the drive IC's datasheet as follows. In the required data is shown, taken from the datasheets of the drive IC and the IGBT.

Table 3-3 The required data for the calculation of the gate resistors

Collection of data for gate resistor calculation			
Gate charge	Q_{gate}	93	nC
Drive IC output first stage	I_{O1+}	2	A
Drive IC output second stage	I_{O2+}	1	A
Drive IC output low	I_{O-}	3	A
Desired turn-on time	t_{sw}	200	ns
Drive IC supply voltage	V_{cc}	15	V
Gate intermediate voltage	V_{ge*}	9	V
Gate-emitter threshold voltage	$V_{GE(th)}$	5.2	V

Turn-on resistor

$$I_{avg} = \frac{Q_{gate}}{t_{sw}} = \frac{93nC}{200ns} \approx 0.5A$$

$$R_{DRp} = \frac{V_{CC}}{I_{O1+}} = \frac{15}{2} = 7.5\Omega$$

$$R_{TOT} = R_{DRp} + R_{Gon} = \frac{V_{CC} - V_{ge}^*}{I_{avg}} = \frac{15 - 9}{0.5} = 12\Omega$$

$$R_{Gon} = 12 - 7.5 = 4.5\Omega$$

Choice of turn-on resistor: 5.6 Ω, 0.25 W

Turn-off resistor

$$R_{DRn} = \frac{V_{CC}}{I_{O-}} = \frac{15}{3} = 5\Omega$$

$$R_{Goff} < \frac{V_{GE(th)}}{C_{RESoff} \frac{dV}{dt}} - R_{DRn} = \frac{5.2}{56p \times 5} - 5 = 13.6\Omega$$

Choice of turn-off resistor: 12 Ω, 0.25 W

Soft shut-down resistor

The soft shut-down resistor should be much bigger than the other two, since it should slowly shut down the IGBT in case of an extreme current flowing through it. No calculation is made to support the decision, only a qualified guess.

Choice of soft shut-down resistor: 330 Ω, 0.25 W

3.6.2.2 Supporting components

Protecting the driver V_s-pin from under-voltage

A zener diode makes sure that the Vs-pin of the drive IC cannot go more than 10 V below the V_{ss} supply voltage. A diode connected in series protects the zener diode when Vs is in its high state.

Protecting the driver from low side IGBT emitter under-voltage spikes

A capacitor between V_{cc} and COM together with a small resistor between the low side IGBT emitter and COM protects the drive IC's COM-pin from under-voltage spikes.

Protecting the IGBTs against gate over-voltage

A 20 V zener diode between the gate and the emitter of each IGBT protects it from a fatal over-voltage. A voltage spike on the gate can cause the IGBT to fail.

3.6.2.3 Power draw from V_{cc}

Required power from V_{cc} at 4 kHz: quiescent (max 2.5 mA), dynamic (11.2 mW, 0.75 mA), dynamic CMOS (1 mW, 0.07 mA), high voltage static losses (max 2.25 mW, 0.15 mA), HV switching losses (1.7 mW, 0.11 mA).

Total: 3.6 mA.

3.6.3   High-side voltage supply options

3.6.3.1 Bootstrap

The bootstrap option uses a capacitor connected between V_b and V_s as seen in Figure 3-11. This method is not optimal since it requires constant switching in order to keep the capacitor charged, because when the upper transistor is conducting the capacitor will discharge. When the lower transistor is conducting the capacitor will be charged up to the drive supply voltage. The bootstrap setup is working satisfactory in the range of tens of Hz to hundreds of kHz[11]. If the converter is required to output DC voltages, the bootstrap option will not work. The main advantages with choosing a bootstrap setup is the ease of use and low cost, the capacitor will also easily follow the voltage up and down through cycles without causing issues to other circuits.

The bootstrap capacitor is charged through a diode, since the high voltage at V_S has to be blocked from V_{CC}, as seen in Figure 3-11. The diode should be able to block the 1200 V used as a design norm in the switching circuit. It should also have a fast recovery time to minimize the charge fed back from the bootstrap circuit to the V_{CC} capacitor.
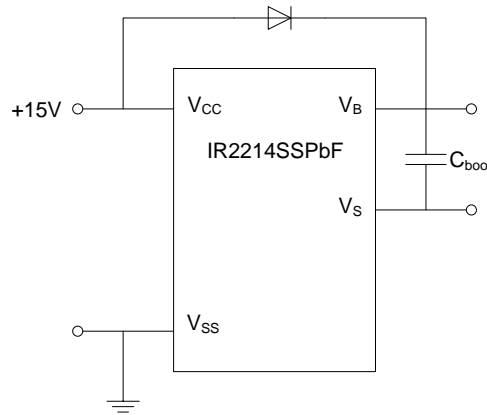

Figure 3-11 Schematics over the bootstrap circuit

The value of the bootstrap capacitor was calculated from the recommendations in the drive IC datasheet as follows

$$\Delta V_{BS} \leq V_{CC} - V_F - V_{GEmin} - V_{CEon,max} = 15 - 1 - 10.5 - 2.2 = 1.3V$$

<div align="right">3-16</div>

where V_F is the forward voltage of the diode, V_{GEmin} is the minimum acceptable gate voltage and $V_{CEon,max}$ is the maximum IGBT forward voltage drop.

$$Q_{TOT} = Q_G + Q_{LS} + \left(I_{LK_{GE}} + I_{QBS} + I_{LK} + I_{LK_{diode}} + I_{LK_{cap}} + I_{DS-}\right) T_{HON} =$$
$$= 93nC + 20nC$$
$$+ (600nA + 800\mu A + 50\mu A + 100\mu A + 0 + 150\mu A) \times 20ms$$
$$= 22.1\mu C$$

<div align="right">3-17</div>

where Q_G is the gate charge, Q_{LS} is the drive IC charge, I_{LK_GE} is the gate leakage current, I_{QBS} is the drive IC quiescent current, I_{LK} is the drive IC leakage current, I_{LK_diode} is the diode leakage current, I_{LK_cap} is the capacitor leakage current, I_{DS-} is the desaturation diode bias current and T_{HON} is the desired maximum on time of the high-side switch, here assumed to be 20 ms or a full 50 Hz wave.

---

[11] (International Rectifier, 2007)

The final value of the bootstrap capacitor then needs to meet the following criteria

$$C_{BOOT} \geq \frac{Q_{TOT}}{\Delta V_{BS}} = \frac{22.1\mu C}{1.3V} = 17\mu F$$

Choice of bootstrap capacitor: Sanyo 25TQC22M, 22 μF, 25 V, 90 mΩ ESR

3.6.3.2 Floating power supply

The power supply should supply the voltage needed by the drive on top of the phase leg voltage V_s. Since V_s is constantly switching during normal operation between 0 and V_{dc}, the power supply must float up and down together with V_s. This puts a large stress on the power supply, making it difficult to implement this solution.

3.6.3.3 Bootstrap with backup battery

A third, unexplored, solution is to use the bootstrap circuit for normal switching operation and then use an external 15 V battery for the rare case DC output is required. The battery should be connected in parallel with the bootstrap capacitor. A great deal of care in the placement and connection of the battery has to take place since it will float to high voltage levels, making sure the high voltage side and low voltage side is still physically separated as much as possible. Every drive IC needs its own battery, since they usually works at different switching patterns.

3.7   Snubber circuit

3.7.1   Snubber introduction

A snubber circuit's purpose is to reduce switching stresses and EMI, by limiting voltage and current peaks and *dv/dt* and *di/dt*. There are many different options available, but the simplest one will be explored here; the RC snubber.

3.7.2   RC snubber

The RC snubber consists of a resistor and capacitor in series, connected in parallel to each transistor, as seen in Figure 3-12. The capacitor will be charged by the current running through the transistor at turn-off, thus lowering the losses in the transistor while limiting the turn-off voltage spike. The downside is that the capacitor will discharge at transistor turn-on, pushing an extra current through the transistor that will increase the turn-on losses. The use of a resistor will cause a loss in the snubber circuit at each switching instance.
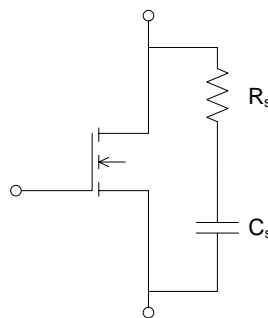

Figure 3-12 Schematics over the RC snubber

The capacitor was chosen by setting the energy lost during turn-off equal to the energy stored in the snubber capacitor according to

$$C_S = \frac{I_0 t_{fi}}{2V_d}$$

where t_{fi} is the current fall time of the transistor, V_d the DC voltage and I_0 is the average current.

The snubber resistance was calculated with the following equation

$$\frac{V_d}{R_s} < I_{rr}$$

<div align="right">*3-20*</div>

where I_{rr} is the reverse-recovery current of the freewheeling diode.

For the simulations a 2 nF snubber capacitor were chosen, in series with a snubber resistor of 100 Ω or 500 Ω, testing two different values.

According to the simulations made, the snubber circuit is not helpful in the current implementation. It's important to note that the real world implementation will have more parasitic elements that are very difficult to estimate which will influence the currents and voltages in the circuit. For this reason a test area for a possible snubber installation is a positive thing, in the unlikely case any component will run outside of its specifications.

A negative consequence of the RC-snubber is the increase in total losses. The results show that the losses in the power transistors are about the same while extra losses in the snubber resistor are introduced. The energy stored in the capacitor is dissipated through the resistor each time it's charged or discharged. At a switching frequency of 2 kHz and with a 2 nF capacitor, a total power loss of 1.5 W is dissipated in the snubber resistor, approximately 50 % of the switching losses of the IGBT at a 10 A load. The switching losses are therefore increased by 50 % by adding the proposed RC-snubber. A much more elaborate snubber is needed to avoid these issues.

3.8   Measurement instruments

3.8.1   Measurement topology

Since the product will be used in a laboratory environment, the testability of it is important. Test pins for easy connectivity of probes and such are described in Section 3.10.6. Furthermore, the input voltage and each output phase current is measured on board, producing analog outputs.

3.8.2   Input voltage measurement

The input voltage is measured by a voltage divider connected to an analog optocoupler to bridge the galvanic barrier. The setup is described in detail in Section 3.4.4.

3.8.3   Input current measurement

An input current measurement circuit was not implemented in the design due to space and usability considerations. To know the input current is simply not important to control an electric machine.

3.8.4   Phase leg current measurement

To efficiently control an electric machine it's crucial to know the current through it, therefore a current measurement module has been place on every output phase. The modules lets the current go through them and the current is then measured by the use of the hall effect, which makes for an accurate and most importantly galvanicly isolated measurement. The chosen device needs 15 V to function and then outputs a voltage signal centered around 2.5 V. A linear relationship between the input current and the output voltage makes for a simple implementation, the following equation describes the relationship

$$V_{out} = 2.5 + 0.0625 i_{phase}$$

Choice of current transducer: LEM HX 10-P/SP2, ± 30 A, +15 V supply, 1 % accuracy, 3 μs response time, 50 kHz bandwidth

3.9 Safety requirements

3.9.1 LVD

Due to the prototype nature of the equipment, it might not be fully compliant with the LVD directive. To make it fully compliant, some form of enclosure of the unit is needed, since the PBA itself is compliant, as well as the documentation.

3.9.2 RoHS

All components on the PBA are RoHS compliant, but the parts were soldered to the PCB with non-RoHS soldering paste.

3.9.3 Insulation standards

During the layout design, the IPC-2221 standard was followed to make sure no creepage currents or flashovers could occur on the PBA.

For the internal layers, the minimum distance between all high voltage conductors was 2 mm at 1200 V.

For the external layers, the components and the component's pads were kept at a minimum distance from each other of 3.635 mm at 1200 V.

3.10 PCB

3.10.1 Board requirements

A large freedom in size and shape of the product is given by the Requirement specification. Other considerations constrict the layout and look more.

1. The board should if possible have a physically separated high voltage and low voltage side.
2. The components around the drive IC should be located as physically close as possible, with special attention on the bootstrap capacitor and the distance to the power transistors.
3. The path running from the drive IC to the gate and back through the emitter leg into the IC creates a loop, which covered area must be kept as small as possible to push the generated inductive circuit to a minimum. Rapid changes in current will induce voltages in this loop that is not wanted, since they can slow the switching speed down and introduce other problems.
4. The connection between the emitter of the high side switch and the collector of the low side switch must be kept as short as possible in order to minimize induced voltages. The very rapid changes in current through this connection will give rise to induced voltages that can cause problems; the output voltage will spike at high side turn-on and drop below negative DC voltage at low side turn-on.
5. If possible, the DC supply lines to the transistors should be made up of copper planes physically located on top of each other to create a capacitor that can counteract the leakage inductances in the circuit and keep the voltage as stable as possible.
6. A large cooler is needed to dissipate the energy lost in the transistors, placement and fixation of the heat sink is important for the structure and usability of the converter.
7. Enough copper in the traces leading the power to and from the converter stages to ensure safe operation within thermal limits.
8. Input and output connectors suitable for lab environment and capable of transmitting the maximum current of the converter (10 A).

3.10.2 Layout

The finished layout is shown in a picture of the PBA in Figure 3-13. The first bullet is address by placing all the low voltage part on the lower half of the card and all the high voltage parts on the upper half of the card. A separation of XX mm is maintained throughout the card. Bridging the gap is optocouplers for control signals to and from the drive ICs and from the voltage measurement circuit. Isolated DC/DC converters are used to transfer energy over the barrier and current transducers measures the output currents with galvanic isolation from the output.

Four identical blocks where built up on the board, facilitating the four channels of the converter. Care was made to place all the components in each block as tight as possible to minimize leakage inductances and provide stable supply voltages. The package with drive IC, support components and high and low side switches, fits within 45 x 40 mm.

3.10.3 Size

The PBA has a size of 300 x 150 mm and a vertical height of 180 mm with the heat sink mounted vertically and the current transducers on the back of the card.

3.10.4 Layers

A four-layer card was chosen to accommodate all the needed wiring, with the middle two layers made with 105 μm thick copper and the outer layers from 35 μm copper. The thick copper in the middle layers are used to rout the power and ground layers, while the thinner copper on the outer layers is used for low voltage power and small signals.
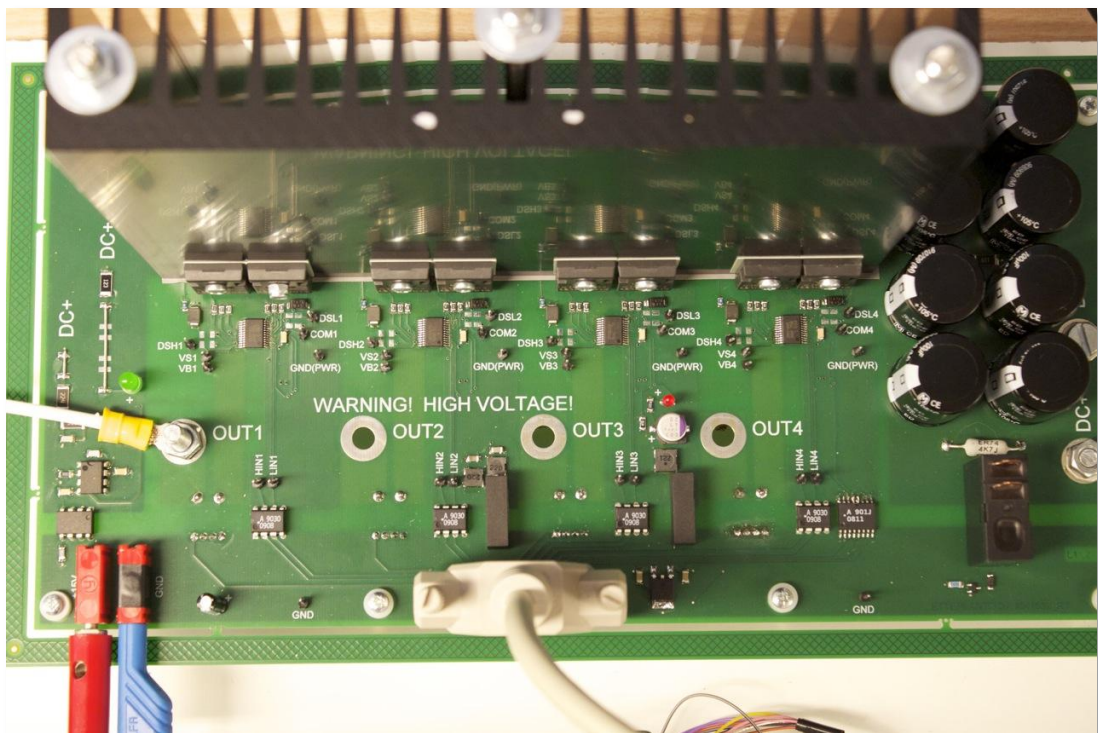

Figure 3-13 Picture of the inverter seen from above

3.10.5 Connections

The PBA has four main connections; two banana contacts for the low voltage input to supply the low voltage circuits (15 V), one 25-pin DSUB connector for all the signals to and from the card, two 6 mm holes for the positive and negative DC power supply and four 6 mm holes for the output.

27

3.10.6 Test points

To facilitate easy testing, test pins were placed around the board, connected to the following points:

- V_B, V_S, $Desat_H$, $Dsat_L$, V_{CC} and V_{SS} for each IGBT-pair
- Fault/SD, SY_FLT
- Control signals to each IGBT

3.10.7 Minimizing leakage inductances

Due to the rapid change in voltages and currents, it's very important to keep leakage inductances to a minimum. By following the recommendations in the data sheet of the drive IC and the points 2-5 in Section 3.10.1 above, the loops and high current paths were minimized.

3.10.8 Cooling solution

Cooling of the IGBTs is covered in Section 3.5.3 above. The other components need no extra cooling. The unit should be able to output 10 A_{rms} without any additional external equipment (i.e. fan) at normal room temperature.

3.11 Description of User Interface

The user interface consists of the various connectors covered in Section 3.4.1, while further description of the measurement circuits is found in Section 3.8. A brief operation instruction follows:

1. Connect all necessary cables (+15 V, DC supply, control system and the load) while keeping the voltage sources turned off
2. Turn on the control system
3. Turn on the low voltage supply
4. Turn on the high voltage supply
5. Start the control system, following these basic steps
   a. When the voltage across the DC bus has reached the desired level (takes approximately 1 s), turn on the relay
   b. Set FLT_CLR high
   c. Start switching (preferably the low side switch first to charge the bootstrap capacitor)
   d. Set FLT_CLR low
   e. The inverter is now ready for operation

3.12 Assembly

The design of the product was chosen to facilitate an open and accessible solution that makes the product easy to move, modify and measure on. Everything on the product is replaceable and customizable by skilled engineers.

The final assembly of the PBA was done by Etteplantech.

3.13 Test and Maintenance

Since the product is a prototype intended for testing purposes, thorough testing is to be done, but maintenance will not be needed, as it will only be used in lab environment and it's highly likely that it will be subject to experiments with different components and therefore maintained.

4   Analysis

4.1   Simulation environment

- OrCAD 16.2
- Simulation models by Infineon

4.2   Hardware verification environment

The hardware verification was done in a laboratory at Chalmers, where DC sources and different loads were readily available.

4.3   Verification Objects

The verified object covered in this report is the printed board assembly, MK1523.

During simulation, two different transistor models were used; a MOSFET model who's most important data is displayed in **Fel! Hittar inte referenskälla.**, and an IGBT with its data displayed in Table 2-2.

4.4   Conclusion

The inverter managed to push a 4 kW induction machine to its limits, both at 4.5 kHz and 18 kHz switching frequency, without any additional cooling. Due to the inductive nature of the machine, the total output energy was 4.9 kVA during testing.

Each phase of the inverter were tested at a continuous output current of 10 A. Although the voltage was only 25 V, it's the current that stresses the IGBTs the most.

The goal of 7 kW of output power was not tested, due to lack of a suitable load.

Only one problem occurred during the hardware testing; the fault sensing signal could not be transmitted to the control system.

4.5   Test overview

The verification starts with the results from computer simulations that were done in order to get a basic understanding of the main components and their operating conditions.

The second phase of the verification was done on the finished hardware, where initial tests to check for errors were done first, followed by calibration of measurement units and finally testing the functionality of the inverter. A summary of the tests and results is shown in Table 4-1.

Table 4-1 Quick overview of the verification tests and its results

Test case	Test method	Notes	Results
Simulation test, MOSFET	A single MOSFET was switched while connected to an inductive load. Tested with both an ideal diode and a second MOSFET as diode.	The aim is to estimate switching and conduction losses in the MOSFET.	With the ideal diode the MOSFET works very well. When the body diode is utilized, a very large reverse-recovery current was pushed through the circuit, causing uncontrollable losses. The CoolMOS type MOSFET is NOT suitable for high voltage inverters!
Simulation test, IGBT	Same test as above, but with an IGBT with an in-package anti-parallel diode.	The aim is to estimate switching and conduction losses in the IGBT.	The results show that the IGBT has higher switching and conduction losses than the MOSFET with the ideal diode, but much lower and controllable losses when utilizing the built-in diode. The IGBT is chosen as the transistor for the inverter!
Simulation test, snubber circuit	Use of same test setup as above with two IGBTs, while adding an RC-snubber circuit across the switching IGBT.	The aim is to evaluate the RC-snubber to find out if it could improve the inverter.	The RC-snubber doesn't notably lower the losses in the IGBT, while introducing extra losses in the snubber circuit. The switching losses in the IGBT are moved from turn-off to turn-on. The only benefit is lower *dv/dt* and hence lower EMC emissions. This type of snubber is not recommended!
Hardware tests, initial tests and calibration	Connection of 15 V low voltage supply, 25 V DC supply. Measurements of input and output currents and voltages.	The tests are done to check for construction errors and to calibrate the voltage and current measurement circuits.	No short-circuits were found. The fault sensor was unfortunately held in fault mode by the optocoupler (held at 5 V while the fault pin needs 15 V). The optocoupler was disconnected. The measurement circuits worked as expected and were calibrated.
Hardware test, bootstrap setup	Testing the bootstrap capacitor maximum duty-ratio, and testing 50 Hz switching.	To make sure the bootstrap capacitor is large and fast enough.	At a switching frequency of 5 kHz, the maximum duty-ratio was 98.75 %. The 50 Hz switching frequency worked perfectly.
Hardware test, current capability	25 V DC voltage, variable duty-ratio, 5 kHz switching frequency and 10 A output.	To test the current capability and make sure the cooling system is adequate.	Each phase could output 10 A, while the IGBTs only became a little hot to the touch.
Hardware test, driving an induction machine	Three phase induction machine was connected to the inverter. 520 V DC in, $f_s = 4.5$ and 18 kHz, $m_a = 1.15$. Thermal imaging analysis.	Testing the main purpose of the inverter. Make sure the temperatures are under control.	The inverter managed to push the 4 kW machine to its limits. At $f_s = 18$ kHz the case temperature reached a maximum 75 °C. The current was approximately 8 A per phase.

4.6   Simulation test 1

4.6.1   Test setup with one MOSFET and one ideal diode

The purpose of this test setup is to get a feeling for the simulation software and the available models. To test the CoolMOS transistors behavior with an inductive load, a step-down converter model was implemented. This model will keep a steady current floating in either the transistor (when it's on) or an ideal diode (when the transistor is in its off state). When the transistor is turned on, the voltage over it is close to zero, and when it's turned off it holds the full DC voltage. By switching between zero and full voltage very fast a mean voltage lower than the input voltage is achieved, thus the name step-down converter. The test setup is shown in Figure 4-1.

The MOSFET model is equipped with a built in temperature model, providing the ability to attach a heat sink model and measure the temperature of the device. The heat sink model used in this simulation is seen in Figure 4-1 and consists of an RC-net. The total thermal resistance is 6 Ω and the ambient temperature is 30 °C. A capacitor of 1 µF is used to simulate the built in heat capacity of the heat sink. The main goal is not to simulate temperatures, so not much time has been spent on the accuracy of the heat sink model or the temperature results.

The drive circuit used is ideal and delivers 15 V during 7 µs and 0 V during 3 µs; the switching frequency was 100 kHz. This is very fast, but helps to keep the simulation times down. The rise and fall times of the flanks are both 10 ns. The gate resistor is only 15 Ω to provide the MOSFET with a large gate current.
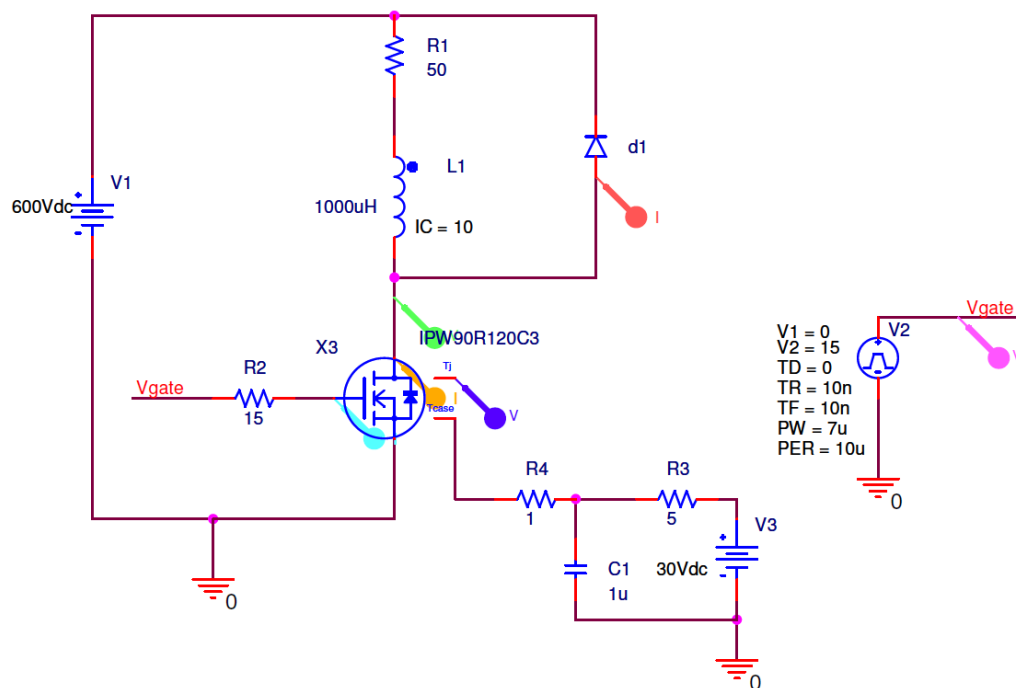
Figure 4-1 Schematics for the test setup in simulation 1

4.6.2 Results

The results were almost as anticipated; nice switching waveforms and fast switching times. Important note on the delay time, as seen in the voltage switching wavetables in Figure 4-2; the turn-off delay is around 1 µs (data sheet specifies 400 ns), while the turn-on delay is around 0.05 µs (70 ns according to the data sheet). This has to be considered in the control algorithms since the duty-ratio of the output signal will be different from the control signal (in this case a control duty-ratio of 70 % was used, but the output duty-ratio is approximately 80 %). The twice as large turn-off delay time has no obvious explanations.
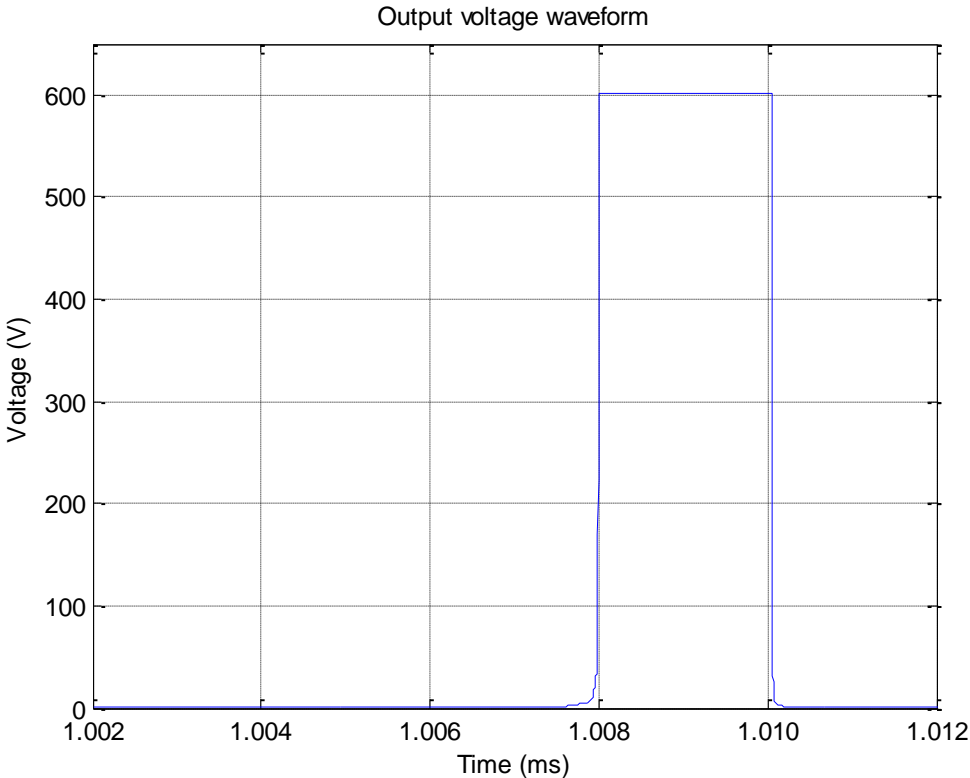
Figure 4-2 Output voltage waveform (MOSFET, ideal diode)
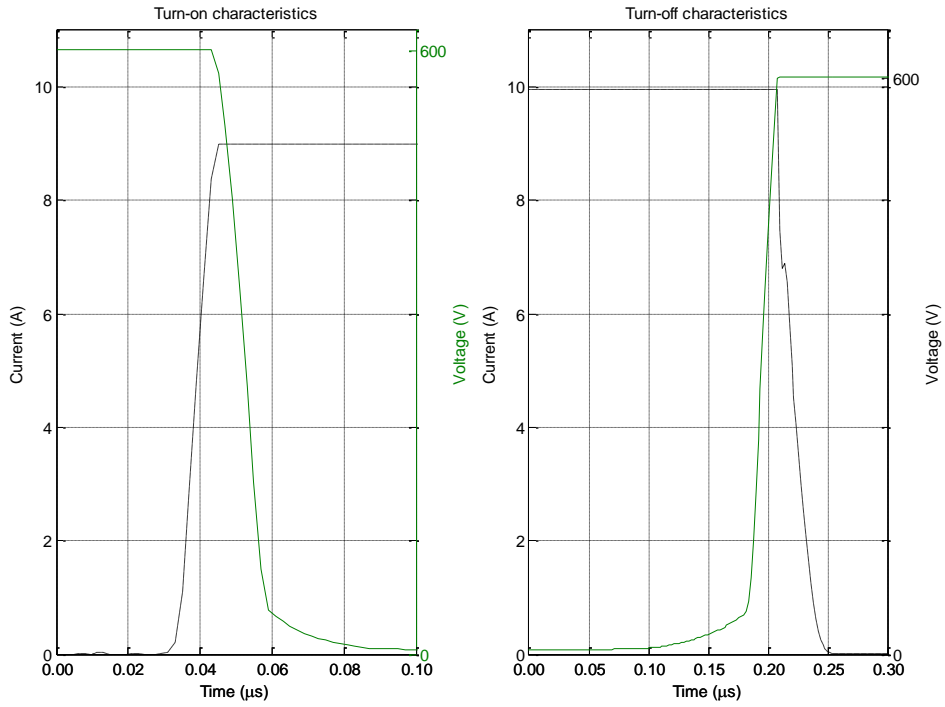
Figure 4-3 Switching characteristics (MOSFET, ideal diode)
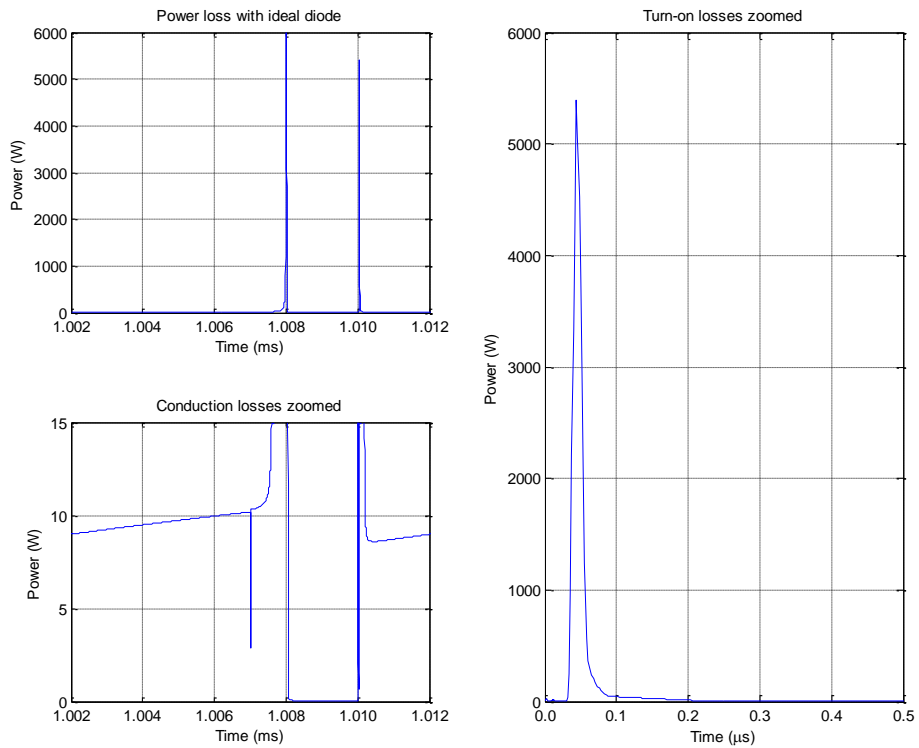
Figure 4-4 Power loss in the MOSFET (ideal diode)

The switching characteristics can be seen in Figure 4-3. Both turn-on and turn-off are according to the data sheet of the CoolMOS. The power produced (and hence lost) in the transistor is shown in Figure 4-4, and the total power loss was calculated to **33.9 W** with the following equation

$$P_{loss} = \frac{1}{T_s} \int_0^{T_s} |V_{ds} \times I_d|\, dt$$

<div align="right">*4-1*</div>

The losses are quite high due to the very fast switching frequency of 100 kHz, since the switching losses vary linearly with the switching frequency, the losses at lower frequencies will be much lower. From the power loss figure, the conduction losses can be approximated to be 9.5 W, and with a duty-ratio of 70% the total conduction losses measures 6.7 W. This shows that from the total losses of 33.9 W, 27.2 W is switching losses (33.9 W – 6.7 W = 27.2 W). Assuming a switching frequency of 2 kHz would instead lead to a total loss of **7.2 W**, with switching losses of only 0.5 W.

4.7 Simulation test 2

4.7.1 Test setup with one IGBT and one ideal diode

- Same test setup as in Section 4.6 above, with the same duty-ratio, switching frequency and drive circuit
- The IGBT model doesn't have the temperature model included. A fixed junction temperature of 32 °C was used.

4.7.2 Results

As in the case with the CoolMOS the results are as expected. The differences between the IGBT and MOSFET technology are also apparent. As seen in Figure 4-5 the turn-off and turn-on delay is approximately 100 ns and 25 ns respectively, giving a output voltage duty-ratio close to the gate duty-ratio of 70 %.

Looking at the switching characteristics of the IGBT, Figure 4-6, the difference to the MOSFET is very apparent at turn-off where the current tail is clearly visible. This elongated current fall time gives rise to a much larger power loss, as can be seen in Figure 4-7. Calculating the total power loss in the IGBT according to Equation 4-1, a total of **137.3 W** of power is lost as heat, 305 % more than the MOSFET. With average conduction losses of (13 W)*70% = 9.1 W, the switching losses account for 128.2 W or 93 % of the total losses. This shows that the IGBT isn't suited for switching frequencies in the 100s of kHz. At 2 kHz the total loss in the transistor is approximately **11.7 W**, which is 60 % more than the MOSFET at the same frequency.
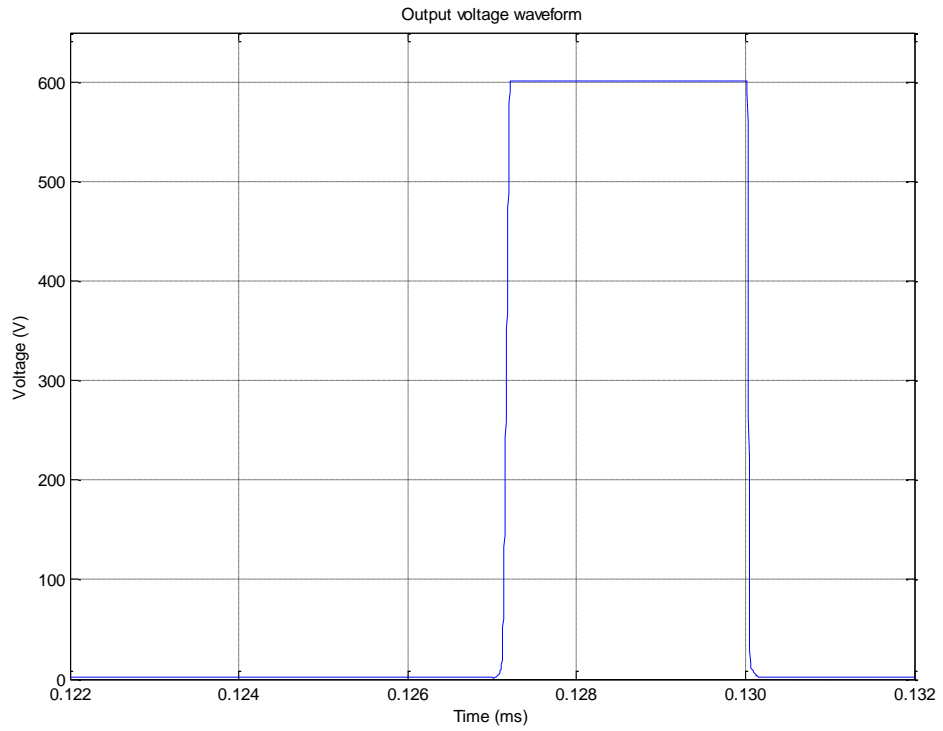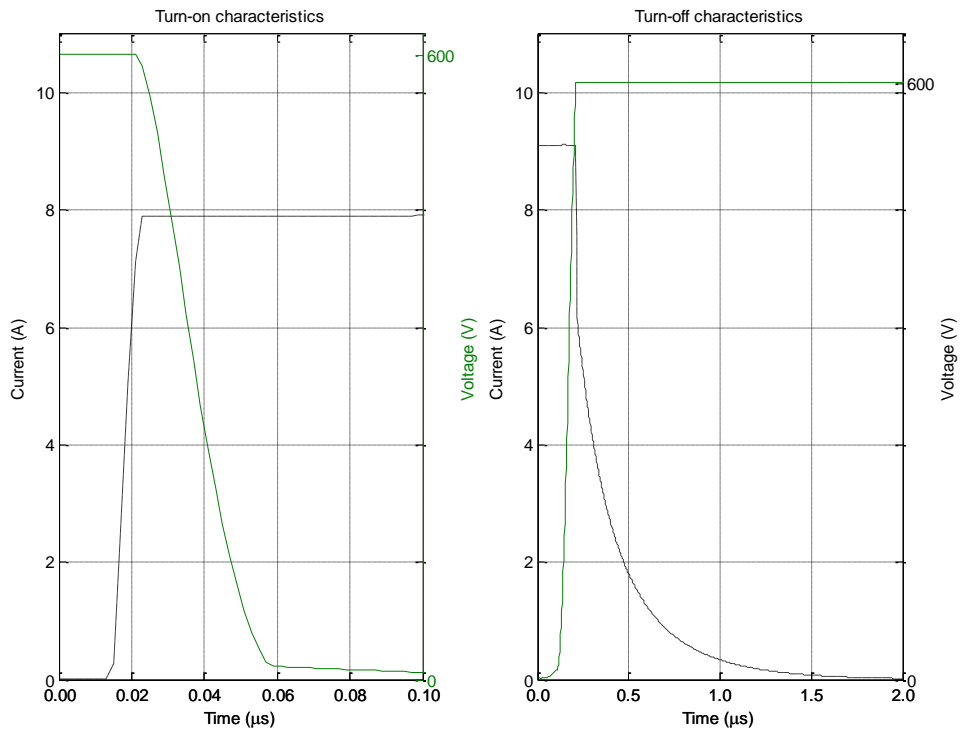
Figure 4-5 Output voltage waveform (IGBT, ideal diode)
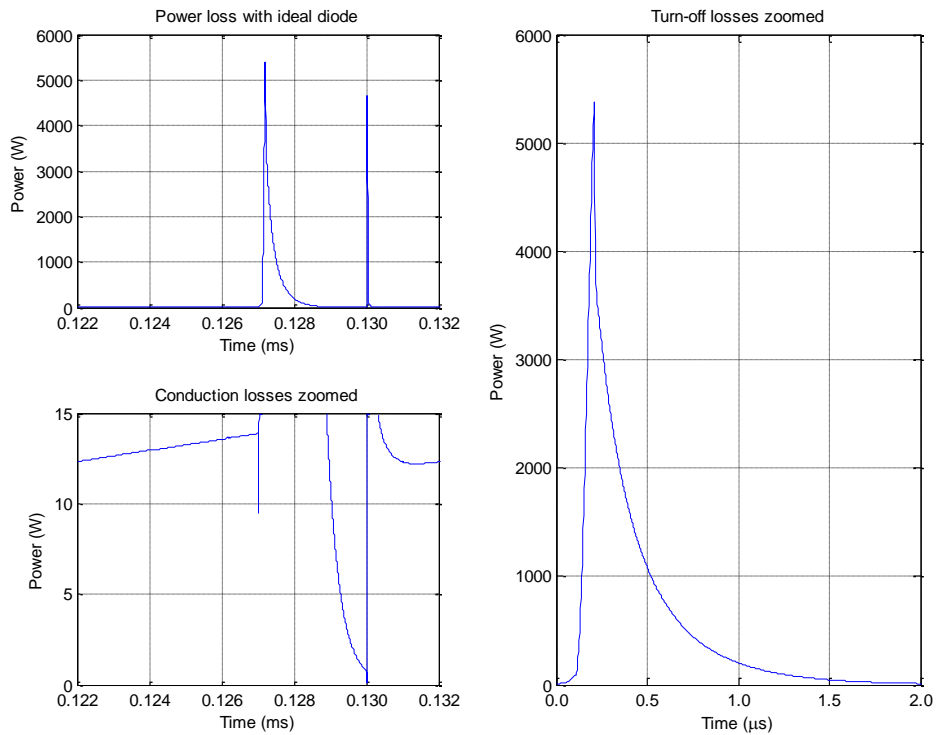

Figure 4-6 Switching characteristics (IGBT, ideal diode)

Figure 4-7 Power loss in the IGBT (ideal diode)

4.8   Simulation test 3

4.8.1   Test setup with two MOSFETs

This test setup is to simulate the behavior of the built in body diode of the MOSFET by replacing the ideal diode in Simulation test 1 by a CoolMOS transistor with the gate directly connected to the source (to keep it in its off-state). As seen in Figure 4-8 both MOSFETs are connected to the same heat sink model.
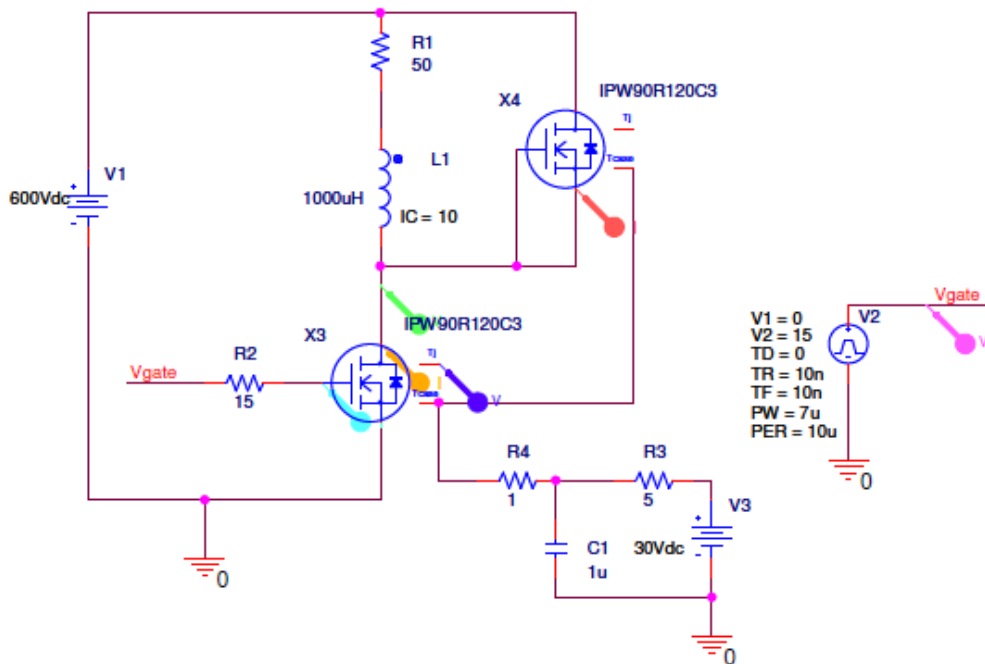
Figure 4-8 Test setup used in simulation test 3

4.8.2 Results

In Figure 4-9 the output voltage waveform is shown. In comparison to the case with an ideal diode, Figure 4-2, a delay in the turn-on phase of the transistor is visible. The switching characteristics are presented in Figure 4-10. When the transistor wants to turn on, the current is passing through the body diode of the upper MOSFET, clamping the voltage to almost zero over the diode. Before the voltage can start to drop, the transistor must take over the current. The problem arise from the very large reverse-recovery current of the built in body diode. At over 80 A, this current must pass through the transistor and hence the power loss in the transistor becomes very high, as seen in Figure 4-11. The large current also cause the voltage delay discussed above by forcing the voltage to stay high until the current has stopped flowing through the body diode.

By integrating the power curve shown in Figure 4-1, the total power loss was found. From the same figure the conduction losses were estimated to be 16.2 W. The total power loss in the switching MOSFET was calculated to be **839.7 W**, which is simply too much for the transistor to handle. The conduction losses in this case are higher than in Simulation test 1 because of the increased temperature caused by the high power loss. Lowering the switching frequency to 2 kHz would bring down the total loss to approximately **32.7 W**, due to the linear nature of the switching losses. It is still very high, but manageable. There is a possibility that the MOSFET will be destroyed during the extreme power levels during the switching, where the power produced in the MOSFET reaches 56 kW during 0.1 µs.

According to the simulations a lower current level will not help the situation, as the reverse-recovery current doesn't seem to have any correlation with the load current. This behavior is very odd and must be due to limitations in the simulation software; normally the reverse recovery current is dependent on the load current.

The conclusion from this simulation is that the CoolMOS type MOSFET is not suitable in the proposed inverter design.
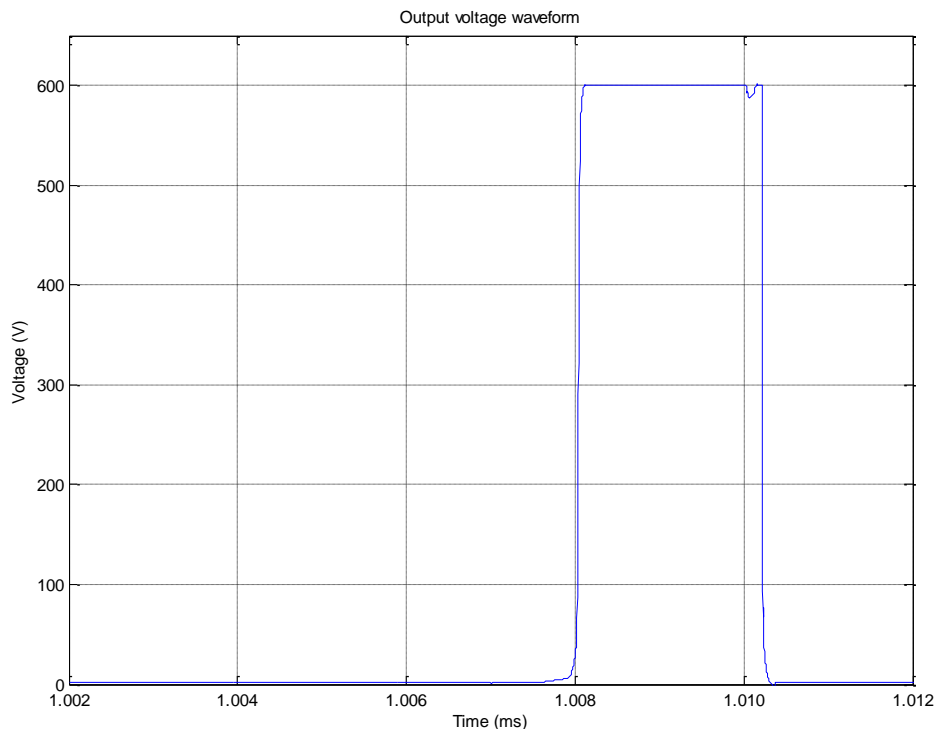

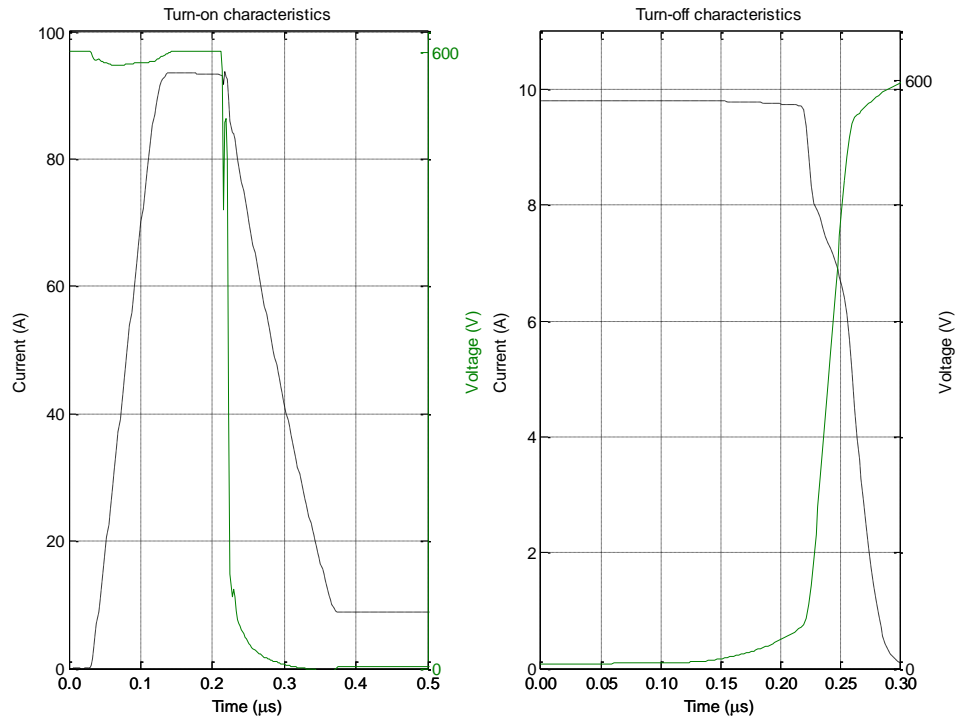*Figure 4-9 Output voltage waveform (MOSFET, body diode)*

37

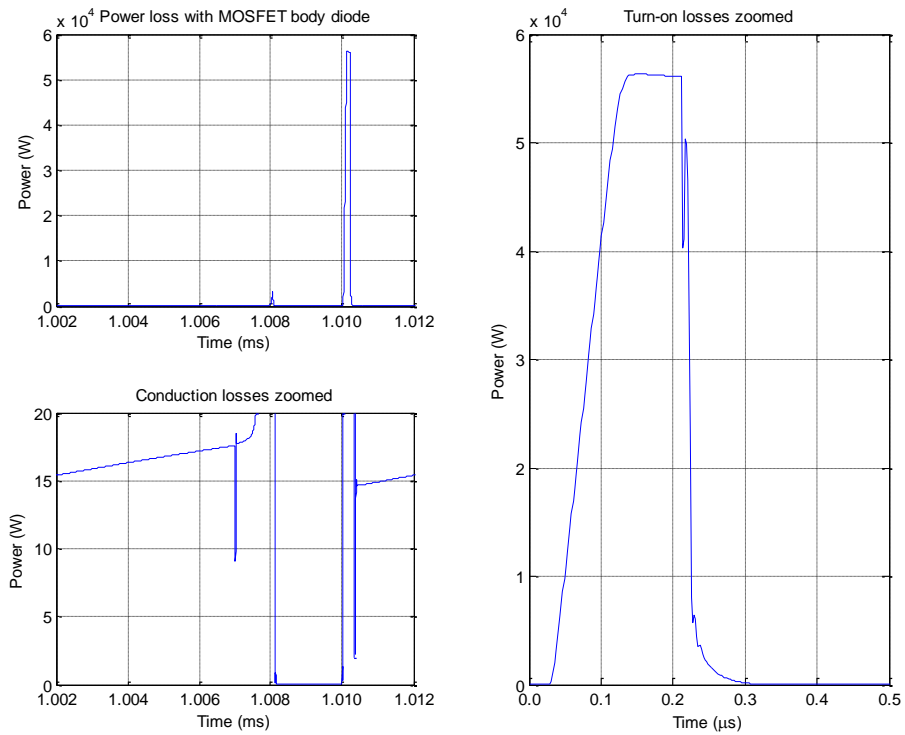*Figure 4-10 Switching characteristics (MOSFET, body diode)*

Figure 4-11 Power loss in the MOSFET (body diode)

38

4.8.3 Modification by adding a SiC diode anti-parallel to the upper MOSFET

A trial to disconnect the built in body diode by connecting a SiC Schottky diode anti-parallel to the upper MOSFET in Figure 4-8 was done to see if it's possible to work around the body diode issues. But as seen in Figure 4-12 this is not possible due to the very low forward voltage of the CoolMOS body diode displayed in Figure 4-13. The CoolMOS diode starts to conduct already at 0.7 V, but the SiC Schottky diode doesn't turn on until 1.5 V according to its data sheet. Thus the body diode is still conducting and the same issues as before are still present.
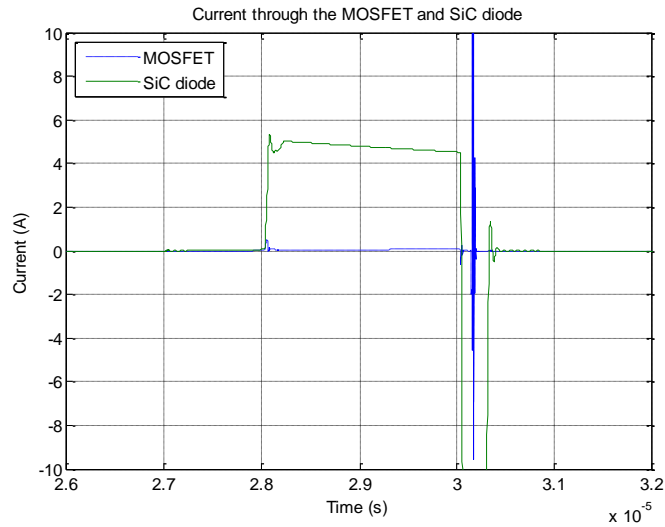
Figure 4-12 Current through the upper MOSFET and SiC diode
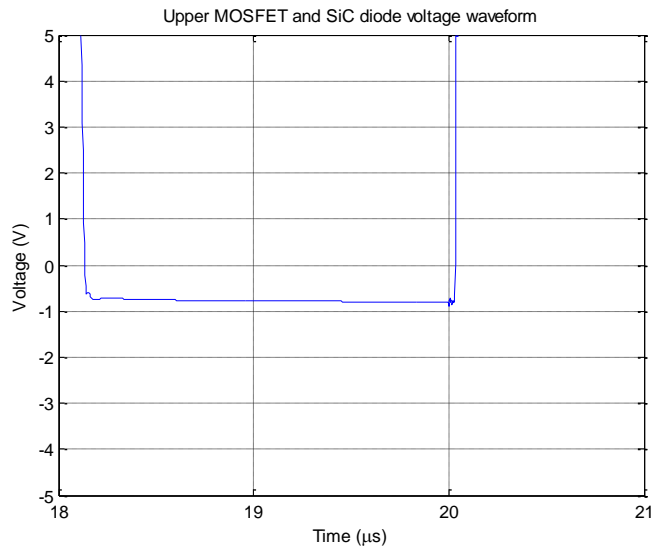
Figure 4-13 Voltage over the upper MOSFET and SiC diode

4.9   Simulation test 4

4.9.1   Test setup with two IGBTs

The purpose of this simulation is to test the built in anti-parallel diode of the IGBT and simulate its effect on the circuit. This test setup represents one leg in a three phase converter during the half cycle when the current is flowing into the leg from the load. Also introduced are leakage inductances to closer simulate the real world situation. Each leg of the transistors has been assumed to introduce an inductance of 10 nH, and the connections to the power source 100 nH. Small resistances have been introduced to aid the simulation software. Other parasitic elements will be present in the real world implementation that is not taken into consideration here because they are very difficult to estimate and are therefore not simulated on the basis of not introducing unknown errors. The test setup is shown in Figure 4-14.

Setup data:

- Switching frequency of 50 kHz, to shorten the simulation times
- Gate resistance of 25 Ω to provide a fast drive circuit
- Gate voltage of 15 V and 50 % duty-ratio
- Rise and fall flanks of 40 and 35 ns respectively to simulate the drive IC
- $V_{dc} = 600$ V, $I_{0(start)} = 10$ A
- Junction temperature of 50 °C
- This test uses the likely main component (the IGBT), hence the implemented parasitic elements is used in this test setup to avoid doing two separate tests
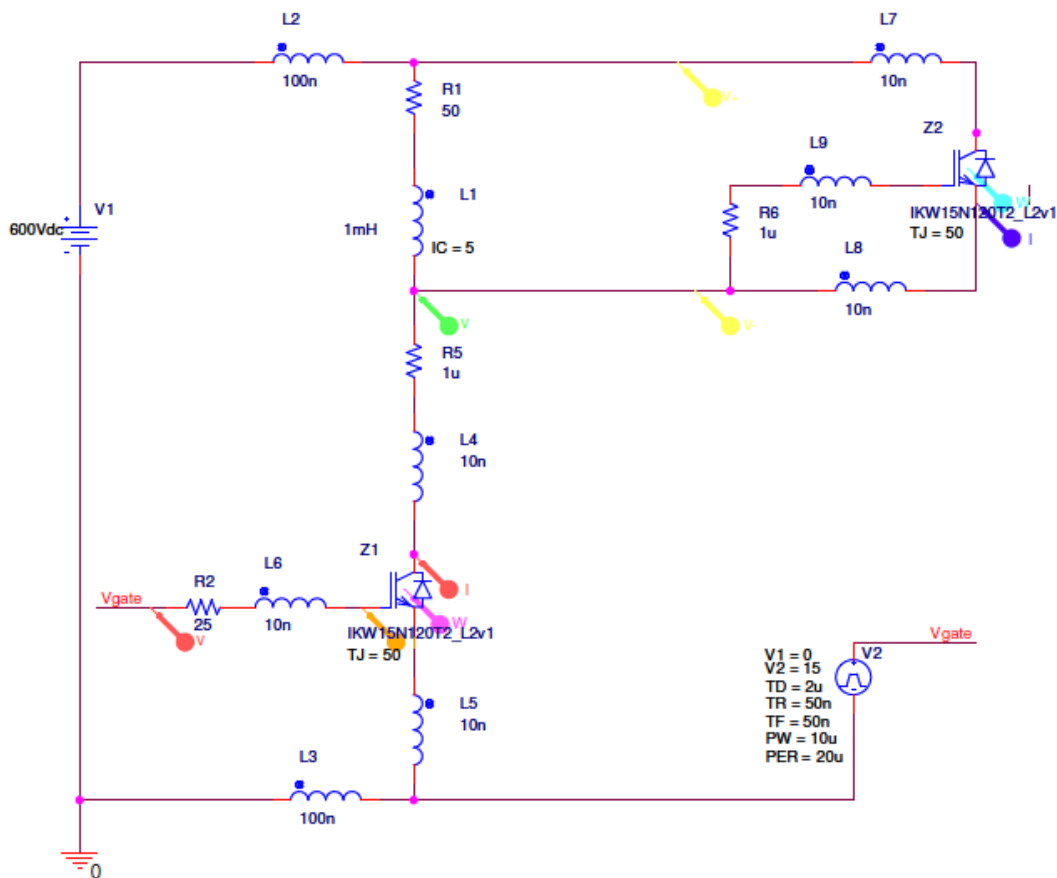

Figure 4-14 Test setup used in simulation test 4

40

4.9.2   Results

As seen in Figure 4-15 the output voltage has some over- and under-shoots at the switching instances. This behavior is due to the leakage inductances who introduce voltage drops when the current through them changes rapidly, according to

$$V_L = L \frac{di}{dt}$$

4-2

where *L* is the inductance and *i* is the current through the inductance. The voltages produced in this simulation are well within the safety margins of the IGBT, one thing to notice is the negative voltage when the transistor turns on which has to be considered in a half-bridge inverter setup. Other than that, the waveform looks good. Other parasitic elements not considered here will influence the result and it has to be assumed that the waveforms will look worse in the real implementation of the product.
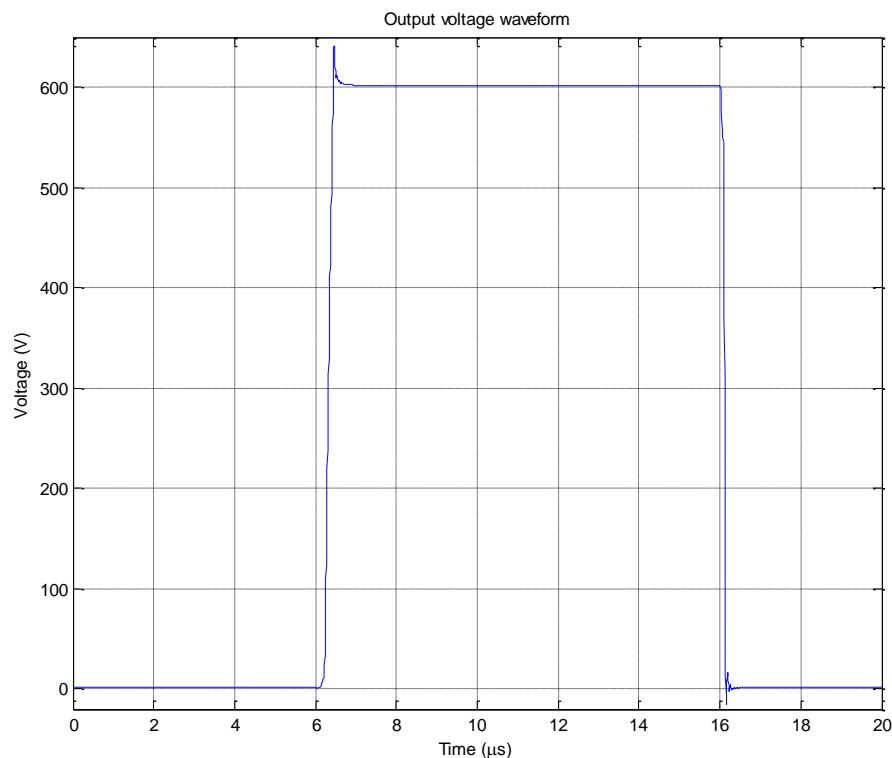
Figure 4-15 Output voltage waveform with two IGBTs and leakage inductances

The switching characteristics are displayed in Figure 4-16 and compared to the earlier results without the parasitic elements there's now some oscillations taking place. The oscillations here are not in any way dangerous to the circuit or the components and should be easily managed. With a turn-off time of 400 ns the turn-off timing is similar to the results in Simulation test 2, even though it should be noted that a slower driver is used in this simulation test. The turn-on timing is a completely different story, as the turn-on time has increased from 40 ns with the ideal diode to 100 ns with the built-in anti-parallel diode of the upper IGBT. This is caused by both the reverse-recovery current of the diode that has to pass through the transistor and the leakage inductances that keeps the current from changing rapidly.
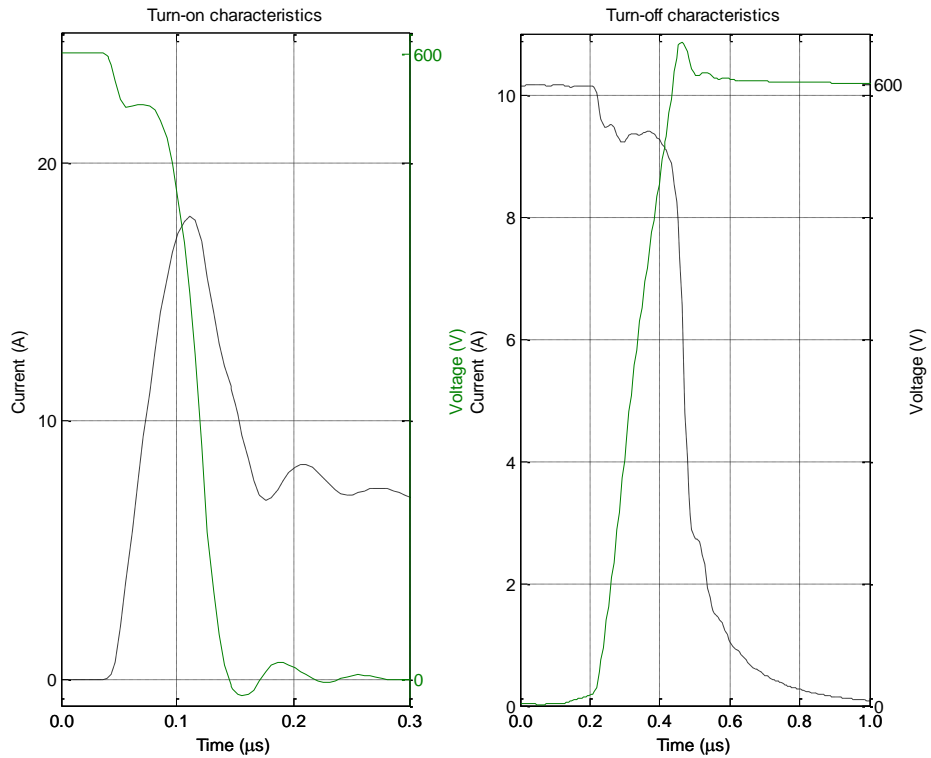
41

Figure 4-16 Switching characteristics with two IGBTs

The loss waveforms for the switching IGBT are show in Figure 4-17. The total losses amount to **81.9 W** at 50 kHz switching frequency. The conduction losses averages to (13.5 W * 50 % duty-ratio) = 6.8 W, and the switching losses then equals 75.1 W. Lowering the switching frequency to 2 kHz would lower the total losses to 9.8 W, actually lower than with the ideal diode in Simulation test 2. This is due to the use of a lower duty-ratio and hence lower conduction losses. The switching losses at 2 kHz are 3 W in this test case and 2.6 W with the ideal diode; 15 % more, due to the reverse-recovery current that is dissipated through the transistor at turn-on and the slower turn-on switch time. There is a dampening effect on the losses due to the parasitic elements causing the voltage at turn-on and current at turn-off to decrease some 5 percent at the start of each switch.
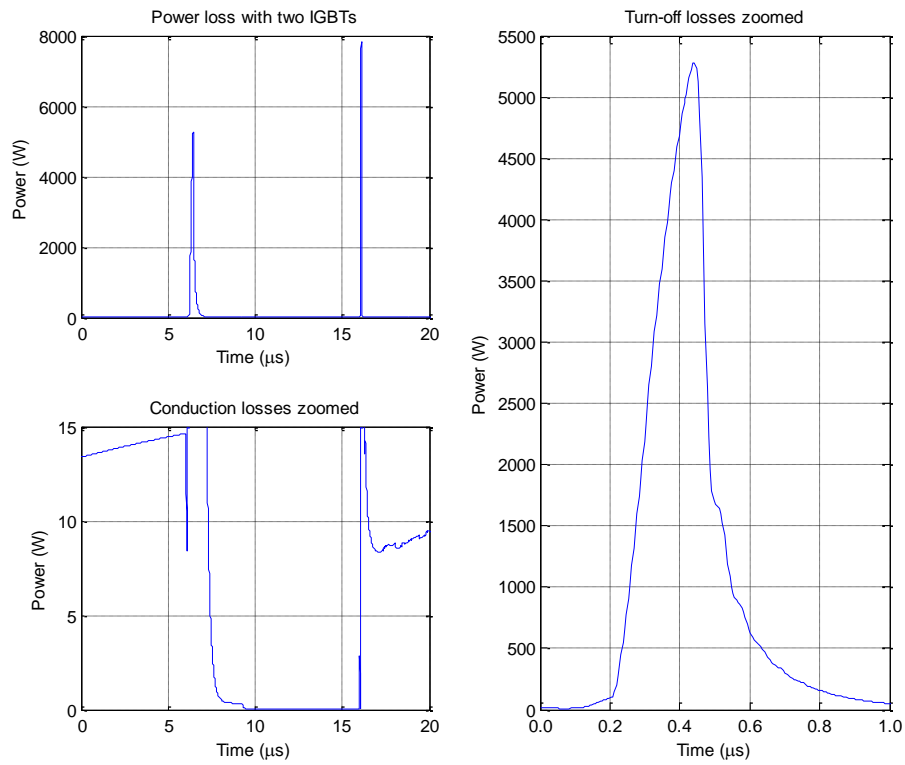
Figure 4-17 Power loss in the IGBT (two IGBTs)

4.10 Simulation test 5

4.10.1 One legged converter with snubber circuit

This test uses the same test setup as in Section 4.9, but adds an RC-snubber over the switching IGBT. Two different valued capacitors and resistors were used, 2 nF and 5 nF, 100 Ω and 500 Ω, giving a total of four variations. The test setup is shown in Figure 4-18.
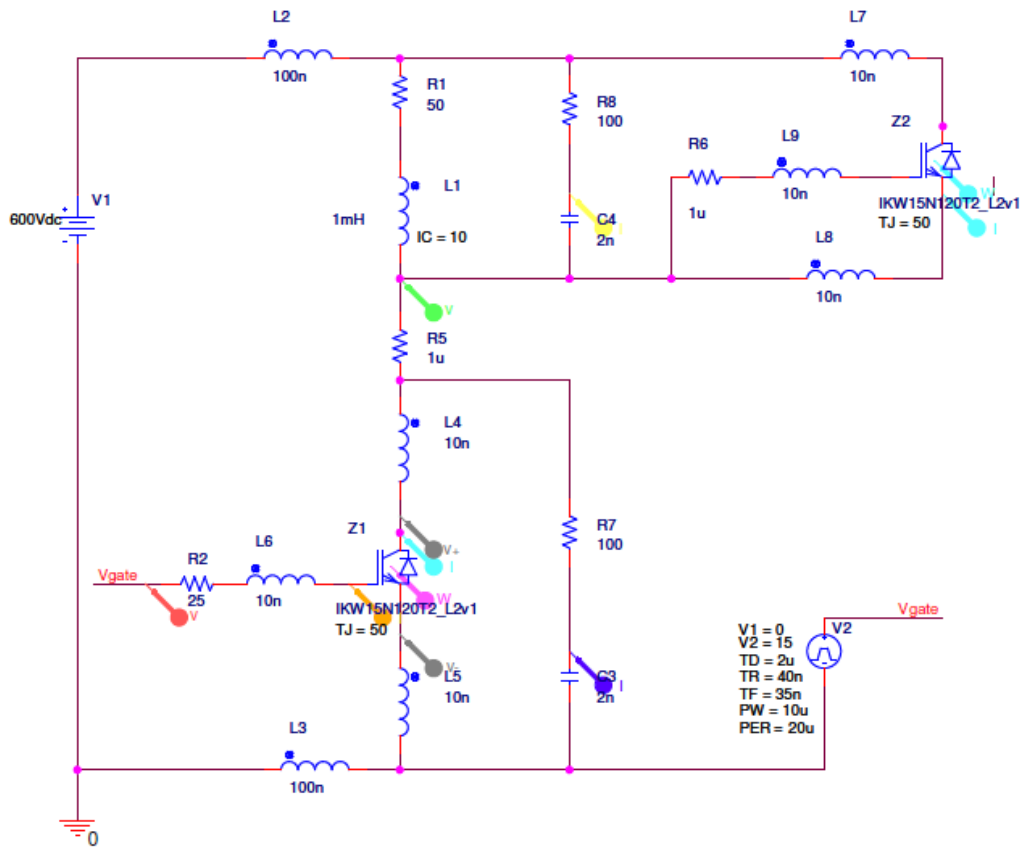
Figure 4-18 Test setup for simulation test 5

4.10.2 Results

Only the results from the 2 nF, 100 Ω case is shown in graphs, since the others are similar in behavior. In Figure 4-19 and Figure 4-20 the power loss during turn-off and turn-on is shown respectively. They clearly display how the power loss are moved from the turn-off event to the turn-on.
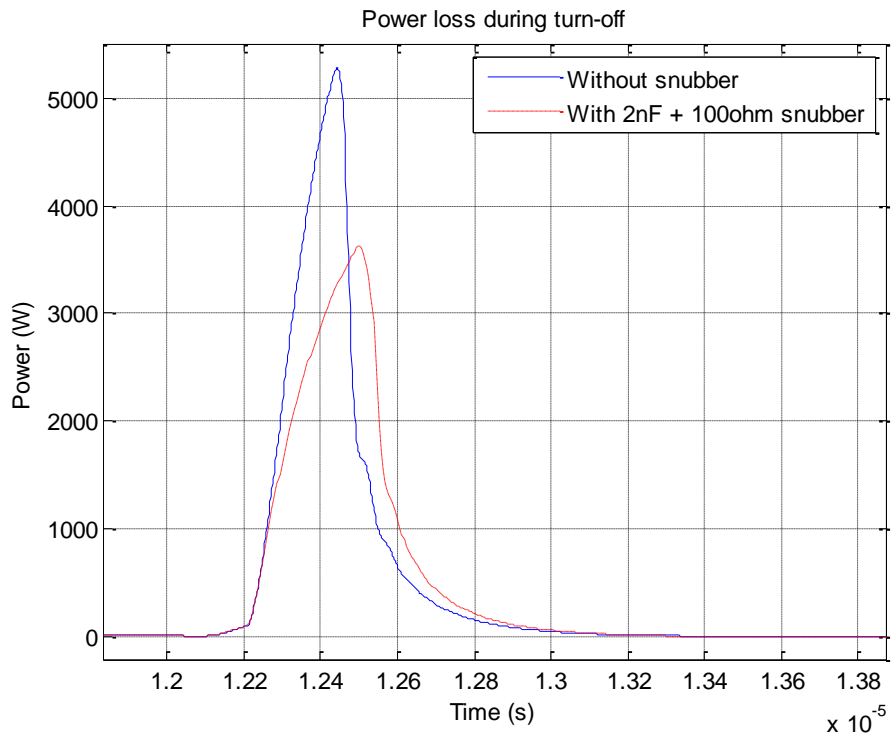
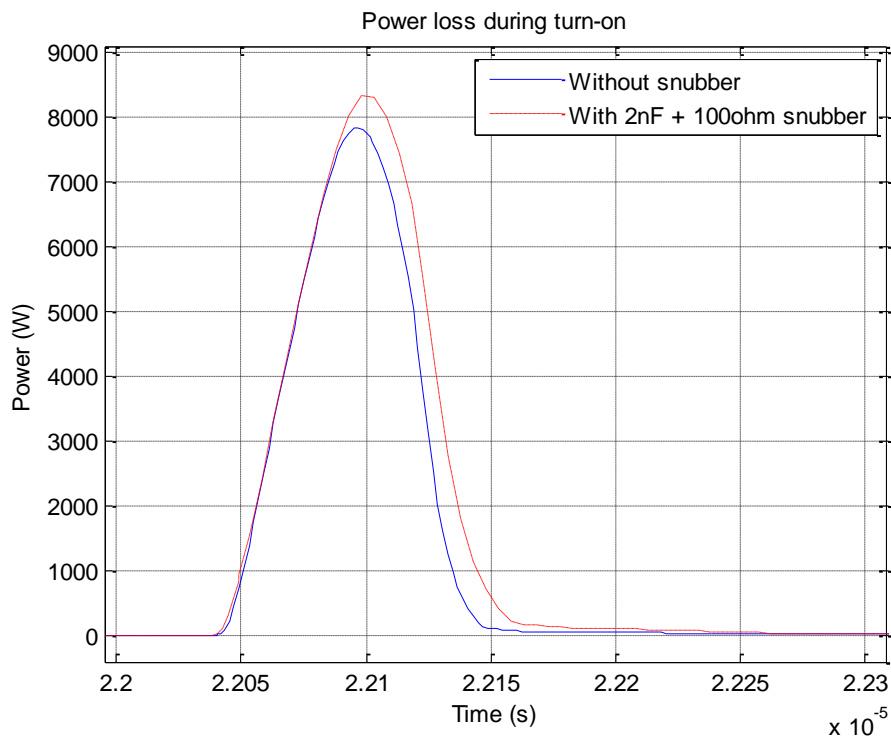*Figure 4-19 Power loss in the switching IGBT during turn-off*

Figure 4-20 Power loss in the switching IGBT during turn-on

The power loss in the switching IGBT for the different cases were calculated to be (using the same method as above):

- 2 nF - 100 Ω: 83.16 W
- 2 nF - 500 Ω: 81.48 W
- 5 nF - 100 Ω: 82.36 W
- 5 nF - 500 Ω: 81.85 W

In Figure 4-21 the voltage curve during turn-off is shown. The snubber clearly lowers the *dv/dt* and shaves of the peak on the voltage spike, as was intended.
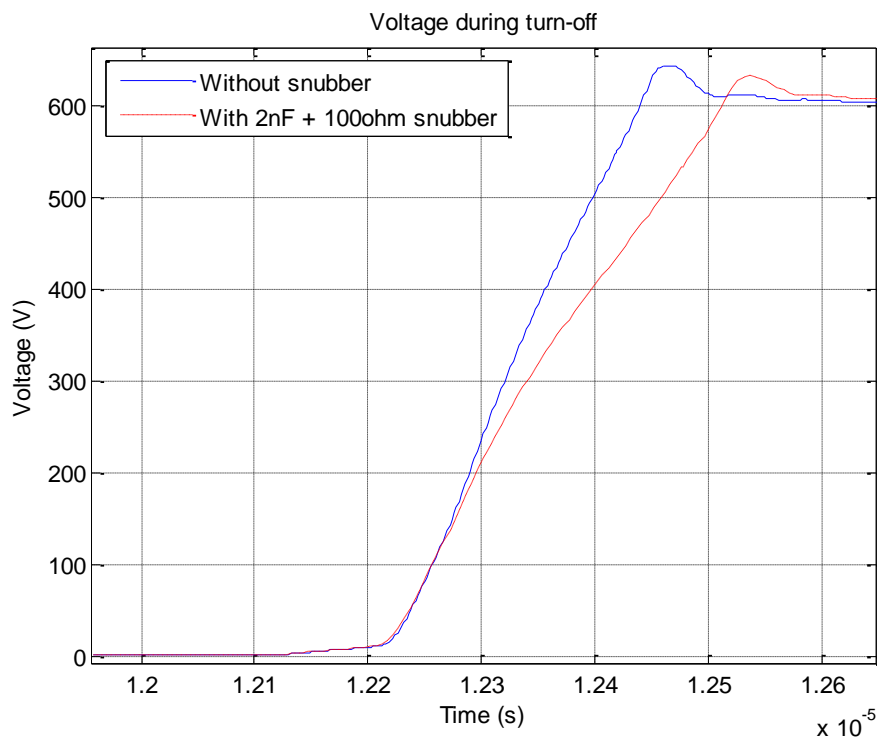

Figure 4-21 Voltage over the switching IGBT during turn-off

The current through the snubber circuit is shown in Figure 4-22, where it's clear how the snubber absorbs the current during the turn-off phase and then pushes it back during the turn-on phase.
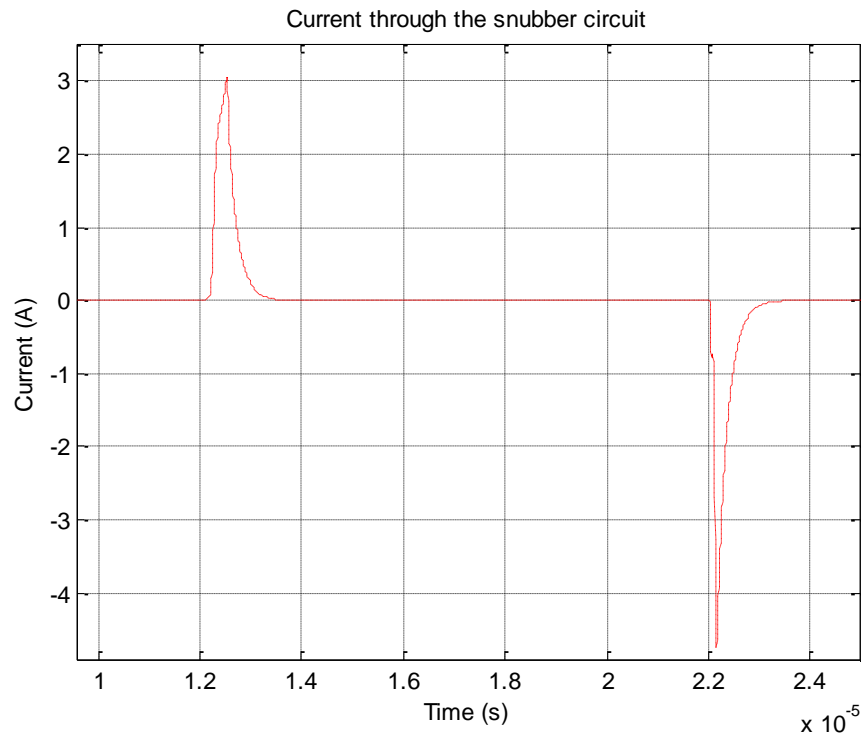
Figure 4-22 Current through the snubber circuit

To conclude, the snubber moves the losses from turn-off to turn-on while lowering the *dv/dt* during switching and shaves of the voltage peak during turn-off. Unfortunately the total losses in the IGBT remains the same, while extra losses are introduced in the snubber circuit, reducing the total efficiency of the inverter. Then the already high current during turn-on is increased even more, possibly causing greater stress on the IGBT. If a reduction in EMC is required, other measures should be tried first, for instance to use higher valued gate resistors to slow down the switching.

4.11 Initial hardware tests

The 25 V-range hardware setup should be used for the initial hardware tests (correct resistors in the voltage dividers).

4.11.1 Low voltage supply short circuit test

Connect a voltage supply to the terminals of the 15 V circuit and slowly ramp up the voltage (with a current limiter in place to make sure nothing will burn), while measuring the current through the circuit. This test is done to make sure that no short circuit is present in the circuit. An estimated maximum current draw of 200 mA should be drawn from the supply, mainly from the current sensors.

4.11.1.1 Result

The circuit drew a constant current of approximately 90 mA and the voltage stayed constant at 15 V. This indicates that the circuit is intact and no short-circuits are present.

4.11.2 Voltage measurement of low voltage circuit

Apply 15 V to the 15 V terminals of the PBA and measure the voltage level of the test points specified in Table 4-2.

4.11.2.1 Results

The results of the measurement are found in **Fel! Hittar inte referenskälla.**.

Table 4-2 Measurement results of the low voltage supply

	Low voltage side	High voltage side
+5 V	5.12 V	5.17 V
-5 V		-5.06 V
+15 V	15.00 V	15.24 V

4.11.3 Test of control signal optocouplers

The input and output signals to and from one of the optocouplers were measured with an oscilloscope. The test was done to analyze the delay and rise/fall time of the optocouplers, while also making sure the control signals reached the drive IC. Only one optocoupler were thoroughly analyzed, while all were tester for functionality. Only the 5 V level were tested, but 3.3 V should work just as well.

4.11.3.1 Results

All the optocouplers worked as expected. The graphs showing the turn-on and turn-off can be seen in Figure 4-23 and Figure 4-24 respectively. The delay is approximately 150 ns, while the rise and fall time of the output signal is actually steeper than the input at 50 ns. This gives the drive IC a good signal to work with.
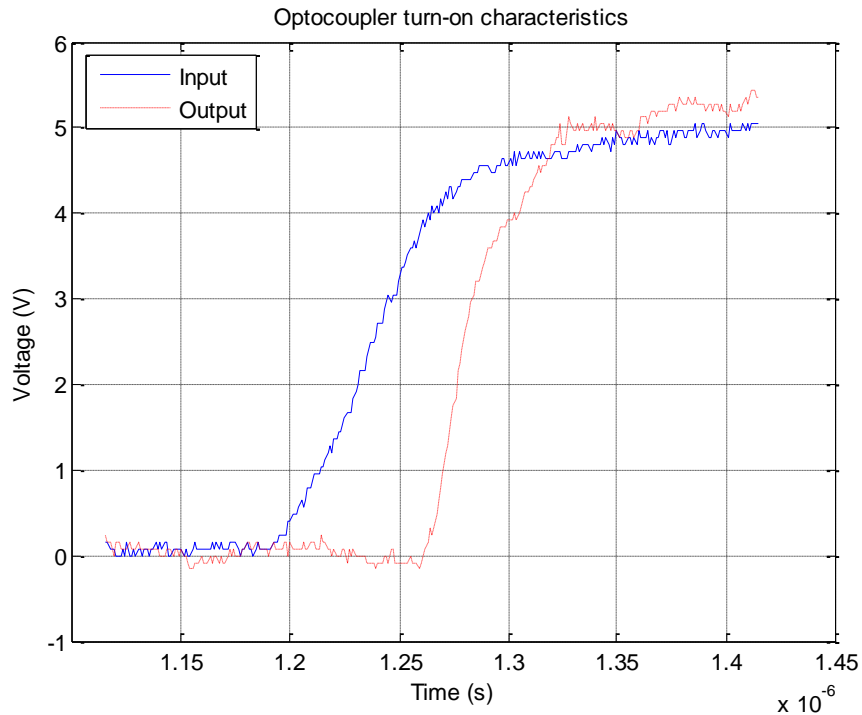

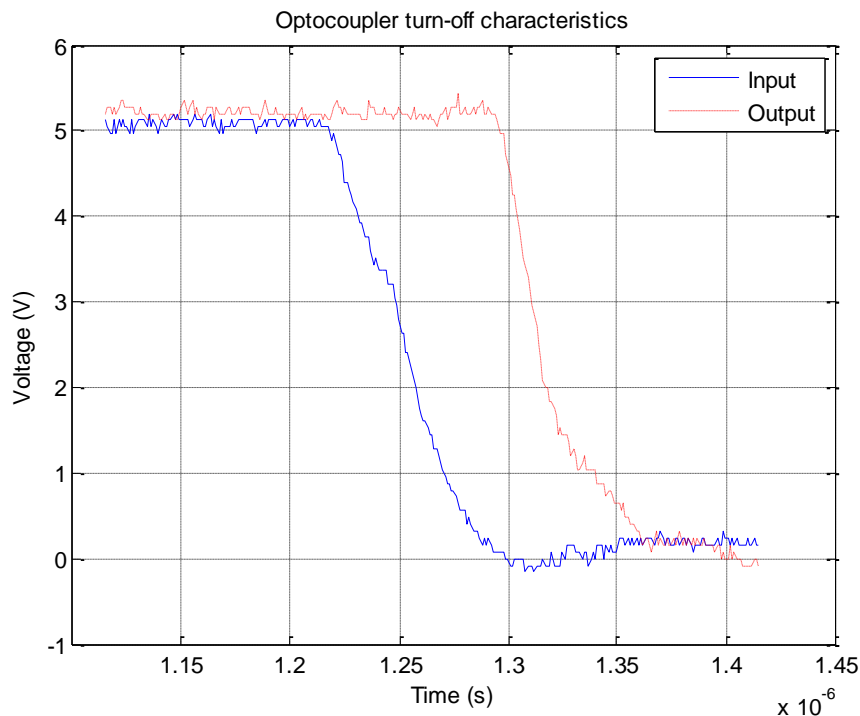Figure 4-23 Input and output signal from one optocoupler during turn-on

Figure 4-24 Input and output signal from one optocoupler during turn-off

4.11.4 Relay test

Apply 15 V to the low voltage terminal and then apply a 5 V signal to the relay control pin and listen for the sound of the relay closing the terminals.

4.11.4.1 Results

The relay clicked and the current draw from the supply terminals rose by approximately 40 mA. The resistance over the relay terminals dropped to zero, measured with a Fluke 77 Series 2.

4.11.5 Short circuit test of DC supply circuit

First apply 15 V to the low voltage terminals and run the gate driver startup sequence (from data sheet), leave all the IGBTs in its open state (i.e. ground all the drive signals). Then slowly ramp up the voltage over the DC supply terminals with a current limited voltage supply while measuring the current. After an initial current to charge the capacitor bank, only the capacitor bank discharge current (approximately 2 mA at 25 V) should flow through the circuit (this current should also light the power indicator LED).

4.11.5.1 Results

The voltage rose without problems to 25 V, while the current draw stayed close to zero amperes. The LED was shining like it supposed to.

4.11.6 Calibration of voltage measurement circuit

Apply 15 V to the low voltage terminals and then apply 5 - 25 V to the DC supply terminals. Measure the output voltage of the linear optocoupler and use Matlab to plot the curve, then use the basic fitting tool to acquire an approximated linear function.

4.11.6.1 Results

The voltage was measured with two Fluke 77 Series 2 instruments. The resulting equation is as follows

$$V_{in} = 10.36 \times V_{out} + 0.07731$$

4-3

and the measurement results is shown in Table 4-3.

Table 4-3 Calibration results for the voltage measurement circuit

Voltage measurements					
V_{in}	5.00	10.00	15.00	20.00	25.03
V_{out}	0.477	0.957	1.437	1.921	2.410

4.11.7 Calibration of current measurement modules

The current measurement modules are calibrated by connecting a voltage source in series with a 10 ohm power resistor on each of the outputs. The low side switch was kept turned on while the high side switch was turned off, 25 V was put on the DC connectors. A current meter was used to measure the current through the resistor and a voltage meter was used to measure the voltage over the output terminals of the current measurement modules, which are rated as follows: $V_{out} = 2.5 + V_{in} * 0.0625$, with the offset accuracy specified to ±50 mV.

Five different currents were sent through each of the outputs in order to get an approximated straight line equation by plotting the curve in Matlab and using the basic fitting tool.

4.11.7.1 Results

Two Fluke 77 Series 2 was used to measure the current and the output voltage. The results are very close to the manufacturer's claims, with only slight deviations from the data sheet values. In Table 4-4 the results are displayed; the approximated constants to the following equation is also in the table

$$V_{out} = A + BV_{in}$$

4-4

Table 4-4 Calibration results for the current measurement modules

I_1	V_1	I_2	V_2	I_3	V_3	I_4	V_4
-1.29	2.437	-1.41	2.417	-1.41	2.424	-1.41	2.416
-0.92	2.461	-0.94	2.446	-0.90	2.456	-0.90	2.447
0	2.518	0	2.505	0	2.511	0	2.504
0.92	2.575	0.93	2.564	0.92	2.549	0.92	2.562
1.29	2.599	1.41	2.594	1.41	2.600	1.41	2.593
A_1	B_1	A_2	B_2	A_3	B_3	A_4	B_4
2.518	0.06251	2.505	0.06287	2.512	0.06232	2.504	0.06289

4.11.8 Test of bootstrap capacitor

The bootstrap construction hinders the high side switch to be turned on indefinitely, hence constant switching is required by the choice of a bootstrap design (the bootstrap capacitor is charged when the low side switch is on, and discharged when the high side switch is on).

Two measurements were carried out, one to measure the highest possible duty-ratio, and one to plot the voltage curve of the bootstrap capacitor.

The first test was done with a single load (a 2 ohm resistor), 5 kHz switching frequency and a DC voltage of 25 V. The duty-ratio was increased until the high side switch could no longer turn on. An oscilloscope was used to measure the duty-ratio.

The second test was done with a differential probe connected to an oscilloscope with an RL load consisting of a 25 ohm resistor and a 40 mH inductor. The DC voltage was 150 V, the switching frequency 50 Hz and the duty-ratio 50 %. This test pushes the bootstrap capacitor in order to test if it's large enough to keep the high side switch turned on during a square wave 50 Hz signal.

4.11.8.1 Results

A Tektronix TDS 2004B oscilloscope and a LeCroy AP032 voltage probe were used during the measurements.

The highest achievable duty-ratio was 98.75%. At this duty-ratio the bootstrap capacitor was charged during 2.5 µs and discharged during 197.5 µs.

In Figure 4-25 the plot of the bootstrap voltage from the second measurement is shown. The charge, and discharge pattern is clearly visible in the figure, were it's important to note that due to the inductive load, the low side switch diode is on, causing a negative voltage drop that slowly decline, hence the declining voltage during the charge phase. The quick drop in voltage (the step in the middle) is caused by the turn on of the high side switch, pulling a larger current to make the switch, followed by a phase when the capacitor is slowly discharged by the small leakage currents in the circuit.

The conclusion is that the capacitor is large enough to hold the voltage high enough over a cycle. It should also be noted that the drive circuit pulls very little energy from the capacitor and that the overall leakages in the drive circuit is low.
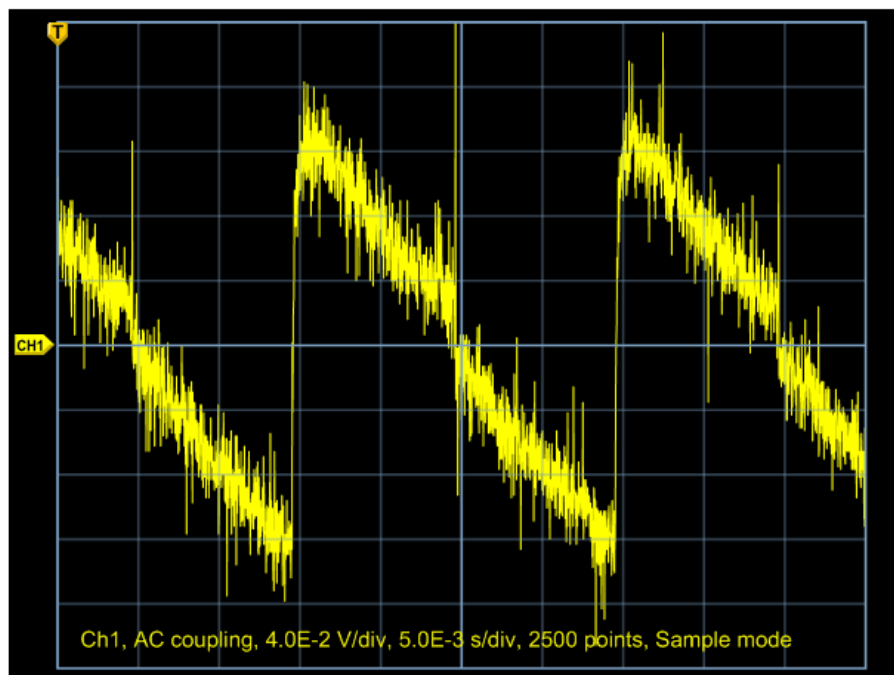

Figure 4-25 Oscilloscope picture of the bootstrap capacitor voltage

4.12   Current test

A 2 Ω, 40 mH load was connected to one phase of the inverter, while the DC voltage was 25 V. The duty-ratio was varied until a 10 A output current was reached. The test should reveal any thermal problems in the design.

4.12.1.1 Results

Each phase of the inverter easily handled the 10 A load, while the IGBTs only became a little hot to the touch.

4.13 Running an induction machine

The inverter was connected to a three phase induction machine to test the output capability of the inverter; the DC voltage was 520 V. Due to the lack of a larger machine, a maximum active power of 4 kW could be absorbed by the machine.

4.13.1.1 Results

The inverter managed to push the machine to its 4 kW limit, both at a switching frequency of 4.5 kHz and 18 kHz, without any additional cooling (at room temperature). Because of the inductive nature of the machine, the total power drawn from the inverter was 5 kVA (the machine had a power factor of 0.8). See Section 4.14 for more details.

4.14 Thermal analysis of the inverter

An induction machine was connected to the first three outputs of the inverter in a Y-connection. A floating, voltage controlled, DC supply powered the inverter on the DC side. For this test a control program that slowly ramped the induction machine from standstill to full speed was used. This was implemented to keep currents and voltages under control, connecting the machine directly to a 400 V, 50 Hz supply can cause currents in the 100s of amperes. During the ramp the machine was un-loaded. After the machine had reached full speed and the voltage had stabilized at the set frequency and voltage, a DC machine was used to brake the induction machine, forcing it to pull more current from the inverter. The control system of the inverter has no feedback; it only outputs a PWM signal to deliver a constant sine wave from the inverter, a control scheme suitable for the test at hand.

While running the experiment, a heat camera was used to take an image of the inverter, showing the hot and cold places of the inverter. Two important results can be extracted from this test; the first to investigate if any part or component is out of its thermal range, the second to estimate the losses in the IGBTs.

To estimate the power losses in the IGBTs the thermal characteristics together with the measured temperature were used. Two sets of data were taken in order to extract the two main components of the losses; the switching losses and the conduction losses. The same output power together with a different switching frequency provides the necessary environment. The two setups can be seen in Table 4-5.
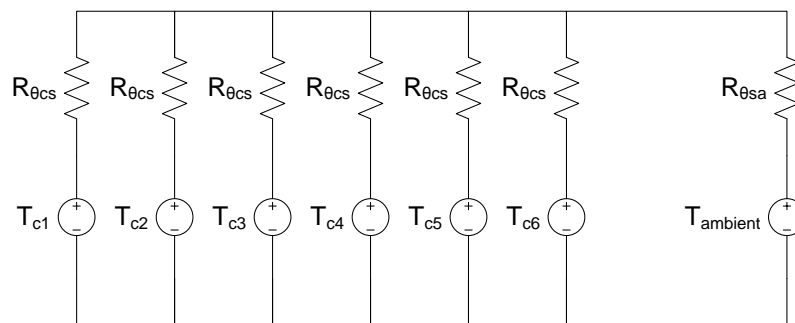

Figure 4-26 The thermal model of the IGBTs and heat sink (case to ambient)

The thermal model of the IGBTs and heat sink can be seen in Figure 4-26. The case temperature is estimated to be the same on all sides of the IGBTs, and the heat sink to have zero inertia. The power developed in one IGBT can then be calculated according to

$$P_{loss} = \frac{T_{case} - T_{ambient}}{R_{\theta cs} + 6R_{\theta sa}}$$

4-5

52

$$\begin{cases} P_{loss,1} = P_{cond} + P_{switch,1} \\ P_{loss,2} = P_{cond} + P_{switch,2} \end{cases}$$

<div align="right">*4-6*</div>

$$P_{switch} = constant \times f_{switch}$$

<div align="right">*4-7*</div>

By combining the equations above, the conduction losses and switching losses of the IGBTs can be estimated. It's important to note that this is a rough estimation with many sources of errors; the thermal model, the large heat sink and the assumptions made about the switching and conduction losses.

To further analyze the results, a measurement of the currents and voltages were done.

<div align="center">*Table 4-5 Test setup for the heat analysis test*</div>

		Test 1	Test 2	
Input voltage	V_{DC}	520	520	V
Switching frequency	f_s	4 500	18 000	Hz
Modulation index	m_a	1.1	1.1	
Output voltage	V_{LL}	350	350	V
Fundamental frequency	f_1	50	50	Hz
Thermal resistance, heat pad	$R_{\theta cs}$	0.4	0.4	K/W
Thermal resistance, heat sink	$R_{\theta sa}$	0.51	0.51	K/W

4.14.1.1 Results

The resulting thermal images can be seen in Figure 4-27 and Figure 4-28. It's clear that the higher switching frequency leads to higher losses, as expected. The maximum temperature at the 4.5 kHz switching frequency was 54.7 °C, and at 18 kHz it was 74.8 °C. In Table 4-6 the results can be seen from the tests, together with the calculated switching and conduction losses.

The assumption made that the temperature of the front casing is the same as the case temperature on the back is most certainly an underestimate of the temperature and therefore an underestimation of the losses. On the other hand the ratio between the conduction and switching losses is more accurate due to the two sampled values.

<div align="center">*Table 4-6 Results of the thermal analysis*</div>

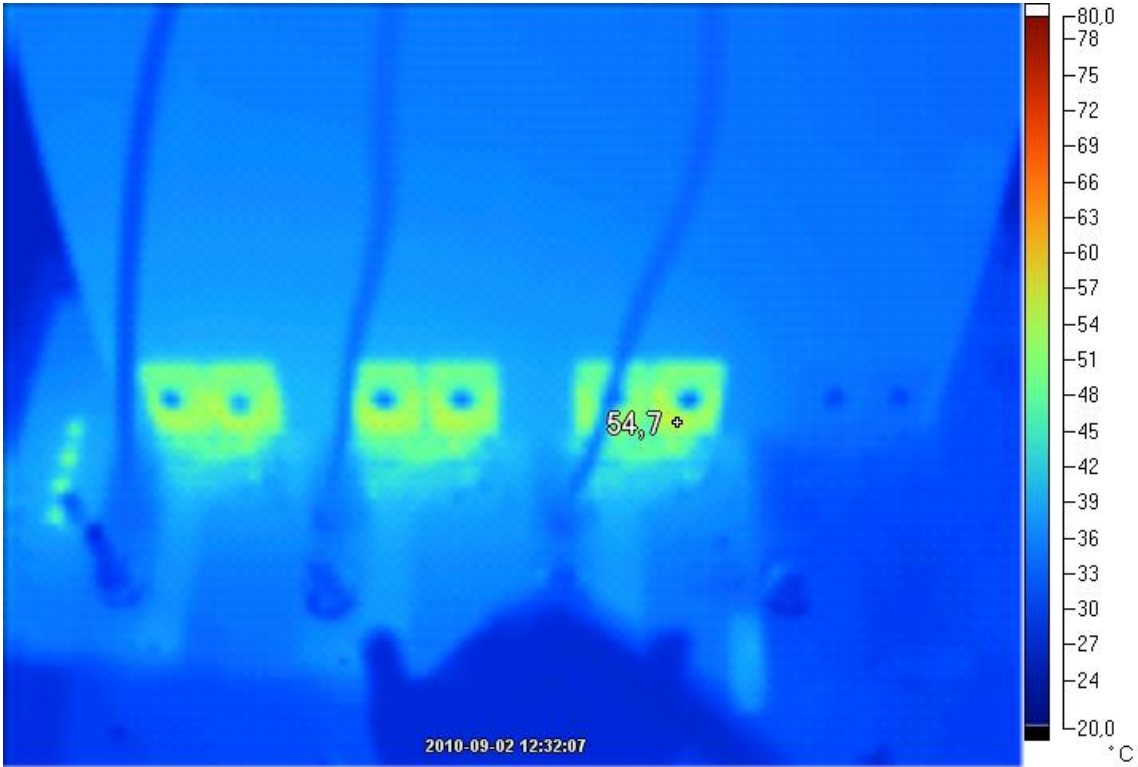| Thermal analysis results		Test 1	Test 2	
Case temperature	T_{case}	54.7	74.8	°C
Ambient temperature	$T_{ambient}$	22	22	°C
Total losses	P_{loss}	9.45	15.26	W
Conduction losses	$P_{conduction}$	7.51	7.51	W
Switching losses	$P_{switching}$	1.93	7.75	W
Output current	I_{out}	~8	~8	A

Figure 4-27 Thermal image of the inverter running at 4.5 kHz
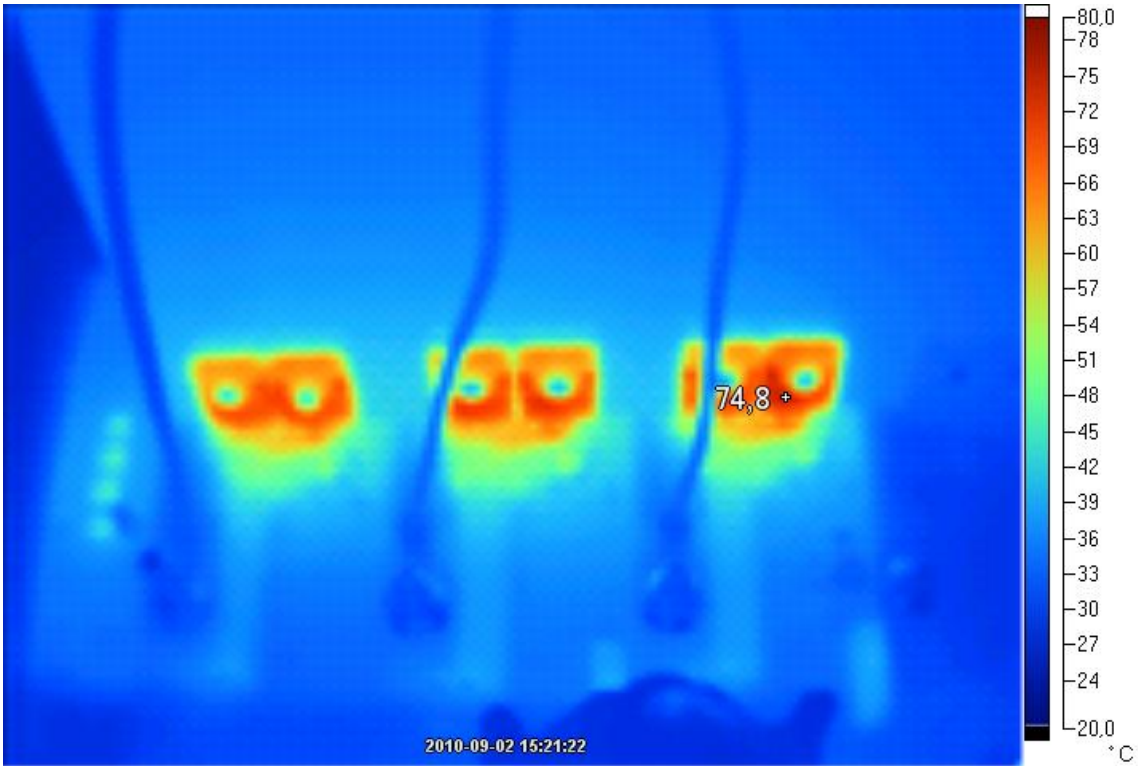

Figure 4-28 Thermal image of the inverter running at 18 kHz

54

4.14.1.2 Conclusion

A straightforward comparison of the losses in the real world experiment and in the simulation above is a little difficult due to slightly different setups. In the simulation the lower switch is studied; it is hard switching at every switch and the output current is more or less constant. In the real world test a 50 Hz voltage is produced, so the current flows in both directions, leading to soft switching in approximately half of the switches (when the current is flowing in the built-in diode, turn-on or turn-off is "soft", since the IGBT is bypassed). This effect could cut the switching losses in half. The conduction losses are also approximately half from the IGBT and half from the built in free-wheeling diode, which have a lower voltage drop and therefore lower losses than the IGBT when conducting. The last hurdle is the average 8 A out of the real inverter, and approximately 9 A in the simulated setup. Also the voltage level was higher in the simulation at 600 V, compared to 520 V in the experiment. Only the current influence the conduction losses, while both current and voltage level influence the switching losses. A factor was used to correct the simulated results to the experiment levels. The conduction losses were multiplied by 8/9ths, while the switching losses were first cut in half due to the "soft switching" and then multiplied by 8/9ths and then 520/600s.

The comparison results are shown in Table 4-7, showing that the simulation results were quite accurate. Therefore the conclusion is that the simulation software together with the manufacturer's models can form a foundation for estimating the losses, and hence the needed cooling, in the finished design.

Table 4-7 Comparison between simulation and real life results

	Simulation	Real life
Current	9 A	8 A
Voltage	600 V	520 V
Conduction losses	6.75 W	7.51 W
Switching losses (4.5 kHz)	6.75 W	1.93 W
Adjusted switching losses	2.6 W	1.93 W
Adjusted conduction losses	6.00 W	7.51 W

4.15 Measuring the switch curves for the high side switch

To see the switching patterns of one of the switches, four things needs to be measured; current through the IGBT, voltage over the IGBT, gate voltage and output current. The most difficult to measure is the IGBT current, since the space is very limited. A small Rogowski type device had to be used, thread around the emitter of the IGBT.

During the test, the DC voltage was held at 300 V, a three phase inductive load was used and a 50 Hz sinusoidal voltage was outputted, while the switching frequency was 5 kHz.

4.15.1.1 Results

The following equipment was used to conduct the measurements:

- LeCroy WavePro 715Zi – Oscilloscope
- LeCroy AP032 – Differential voltage probe
- LeCroy AP015 – Current probe
- PEM CWT 015B UM – Rogowski current transducer

In Figure 4-29 and Figure 4-30 the switching curves during turn-off and turn-on is shown. The curves are very similar to the curves from the simulation above, Figure 4-16, and nothing out of the ordinary was to be found. The turn-off time is approximately 400 ns, including a delay of 100 ns.

The turn-on was much faster at approximately 100 ns. Here the reverse-recovery current from the low side IGBT module is clearly shown, more than twice the output current flows through the high side IGBT during approximately 100 ns, causing the switching losses to increase. The times two ratio is very close to the one found in the simulations above.

During turn-off the *dv/dt* is approximately 1 V/ns, while at turn-on it's 2.5 V/ns. The change in current, *di/dt*, at turn-off is approximately 7 A/µs, and at turn-on 50 A/µs.

The results should scale well with voltage and current, though extreme values could reveal a phenomenon not visible here.
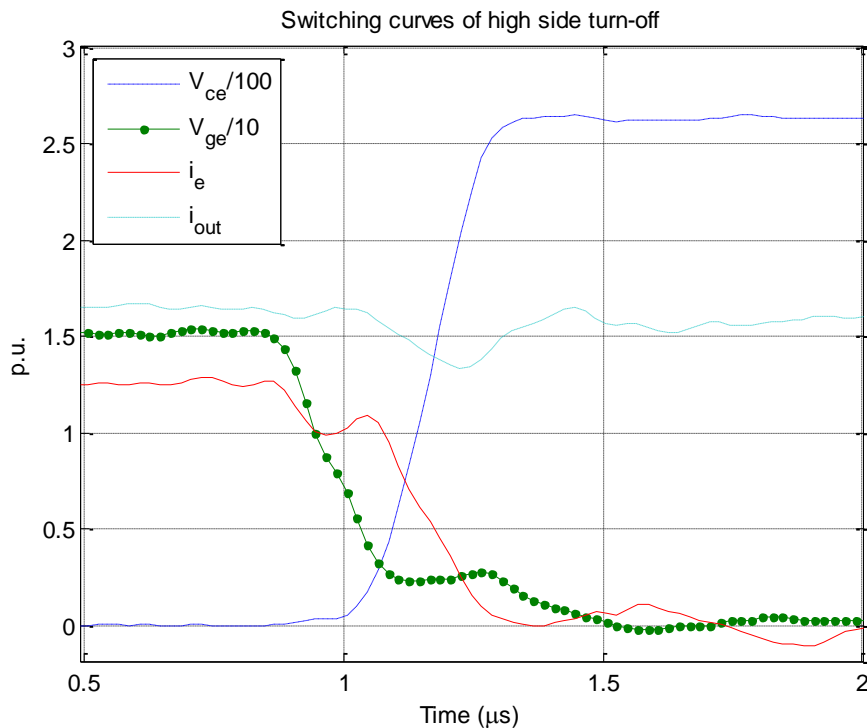
Figure 4-29 Switching curves of the high side IGBT during turn-off
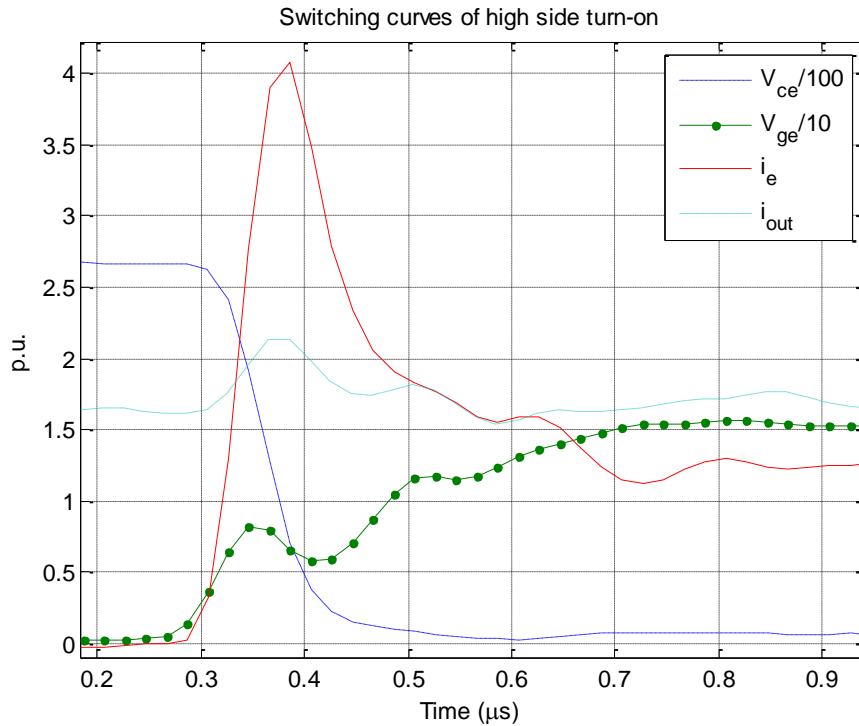
Figure 4-30 Switching curves of the high side IGBT during turn-on

4.16   Wire bound EMI analysis

To measure the influence of the inverter on the net it's connected to, the inverter can be connected to the net through a LISN device (Line Impedance Stabilization Network). With this device an oscilloscope can be used to measure the EMC, while making sure that any interference from the net is not influencing the measurements.

Two sets of measurements can be taken to examine the effect of a snubber circuit over the IGBTs. First a measurement without any snubber circuits and then a measurement with one of the proposed snubbers from above.

Another possible experiment is to test two different sets of gate resistors, changing the switching speed and the *dv/dt* and *di/dt* of the circuit, thus changing the generated EMI.

For this test a thermal analysis would also be needed to investigate the influence of the snubber/gate resistors on the power losses in the IGBTs.

4.17 Efficiency calculation

Knowing the efficiency of the inverter is interesting in order to make a model of it so that the optimum working point in future uses of the device can more easily be found.

There are different ways to measure the efficiency of the device. The most straightforward method is to measure the voltage and current into the device and the voltage and current out of it. The difficulty with this approach is that the accuracy of the measurements needs to be very high, because the efficiency of the inverter is so high, close to 100 %. The waveforms are not ideally formed sine, square or constant either, causing further problems with accuracy.

Another way to measure the efficiency is to use a known and calibrated load and do a thermal analysis of the load to accurately acquire the load power. The input power is then measured with a voltage and current meter, since they are more constant in nature and therefore easier to accurately measure.

Ideally, four different working points should be used to get an accurate model of the inverter; two different switching frequencies and two different loads.

5   Conclusion

The goal of designing and building a four phase inverter was a success. The inverter managed to drive a 4 kW electric machine with switching a frequency of up to 20 kHz. The inverter worked as expected throughout testing, although the limits of the inverter was never found since a large enough machine was not readily available for testing.

During the simulations it was first found that the CoolMOS type MOSFET is not suitable for the type of inverter used in this project. The second conclusion is that the proposed RC-snubber isn't of much help, other than a last stop remedy to reduce EMI if no other option exists, due to the added losses and complexity while not in any meaningful way reducing the stresses on the IGBTs.

The choice to use the bootstrap design for the high side switches proved to be a good one; switching frequencies from 50 to 20 000 Hz were tested successfully. The chosen capacitor, of a solid electrolytic chip type, also proved to be the right choice; fast enough and higher reliability compared to ordinary electrolytic capacitors.

Finally the results from the simulations and the hardware tests proved that the simulation software is a good tool during the design process that could help evaluate electrical and even thermal characteristics of the design or of specific components.

6   Future work

Since the main focus of the project was on the design and production of the hardware, not much time and energy was spent on doing measurements and testing various cases. For example the produced EMI of the invert would be interesting to measure, together with the influence of the RC-snubber on the EMI performance and the total losses.

Further testing to evaluate the robustness of the inverter would also be of interest; short-circuit tests (to test the built-in fault sensing), over-voltage tests and over-current tests.

Another big topic is the control of the inverter and of the electric machine, an area much too wide to be covered in this project.

7 Sources

Infineon Technologies AG. (September 2008). *Infineon Technologies AG.* Hämtat från http://www.infineon.com/dgdl/IKW15N120T2_Rev2_1.pdf?folderId=db3a304412b40795011 2b408e8c90004&fileId=db3a304412b407950112b426d2d43acd den 27 April 2010

Infineon Technologies AG. (2008, July 30). *Infineon Technologies AG.* Retrieved April 26, 2010, from http://www.infineon.com/dgdl/IPW90R120C3_1[1].0_PCN.pdf?folderId=db3a3043156fd573 0115c736bcc70ff2&fileId=db3a3043183a955501185000e1d254f2

International Rectifier. (2007, 03 23). HV Floating MOS-Gate Driver ICs. El Segundo.

Mohan, N., Undeland, T., & Robbins, W. (2003). *Power Electronics.* John Wiley & Sons, Inc.

Premier Farnell. (n.d.). *Farnell Sverige.* Retrieved April 27, 2010, from http://se.farnell.com/infineon/ikw15t120/igbt-n-1200v-15a-to-247/dp/1471745?Ntt=IKW15T120

Premier Farnell. (n.d.). *Farnell Sverige.* Retrieved April 27, 2010, from http://se.farnell.com/infineon/ipw90r120c3/mosfet-n-to-247/dp/1664087?Ntt=IPW90R120C3

Vishay Semiconductors. (2005, March 24). *Linear Optocoupler, High Gain Stability, Wide Bandwidth.* Retrieved June 01, 2010, from Vishay Semiconductors: http://www.vishay.com/docs/83622/83622.pdf

Appendix A

Layout and PCB figures
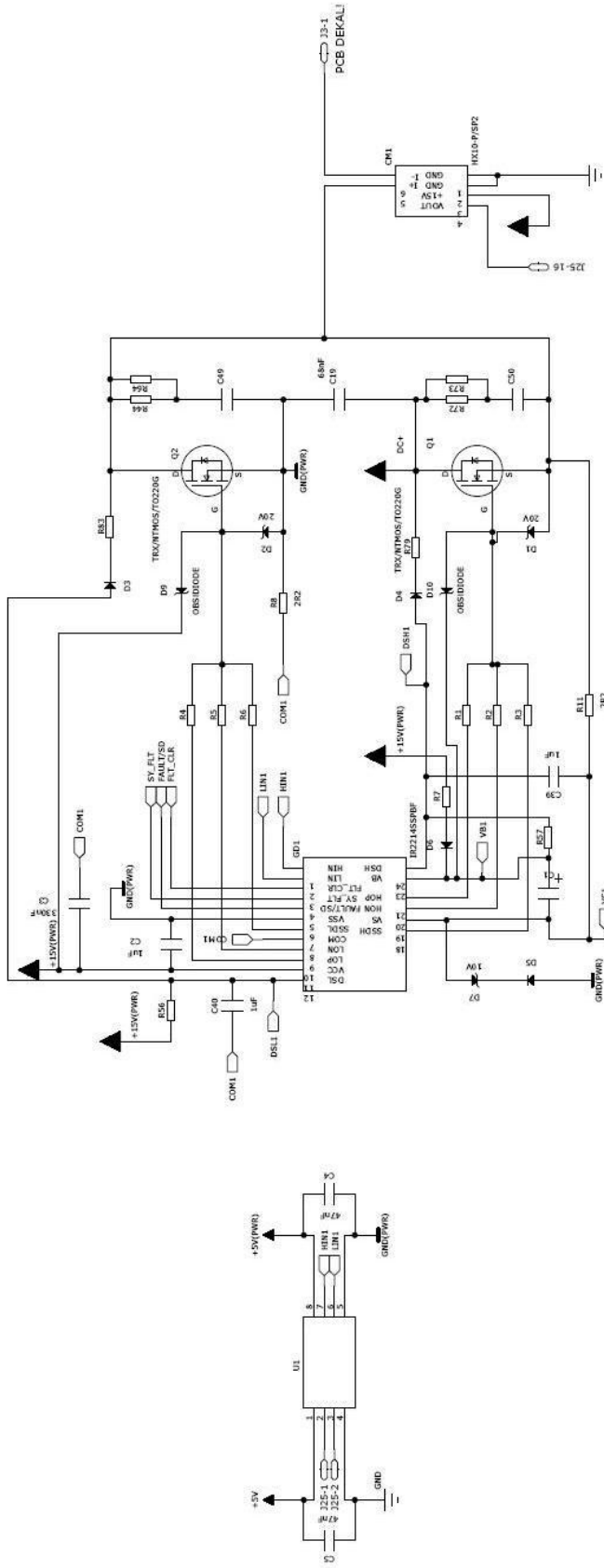
Figure 7-1 Schematics over the first inverter leg
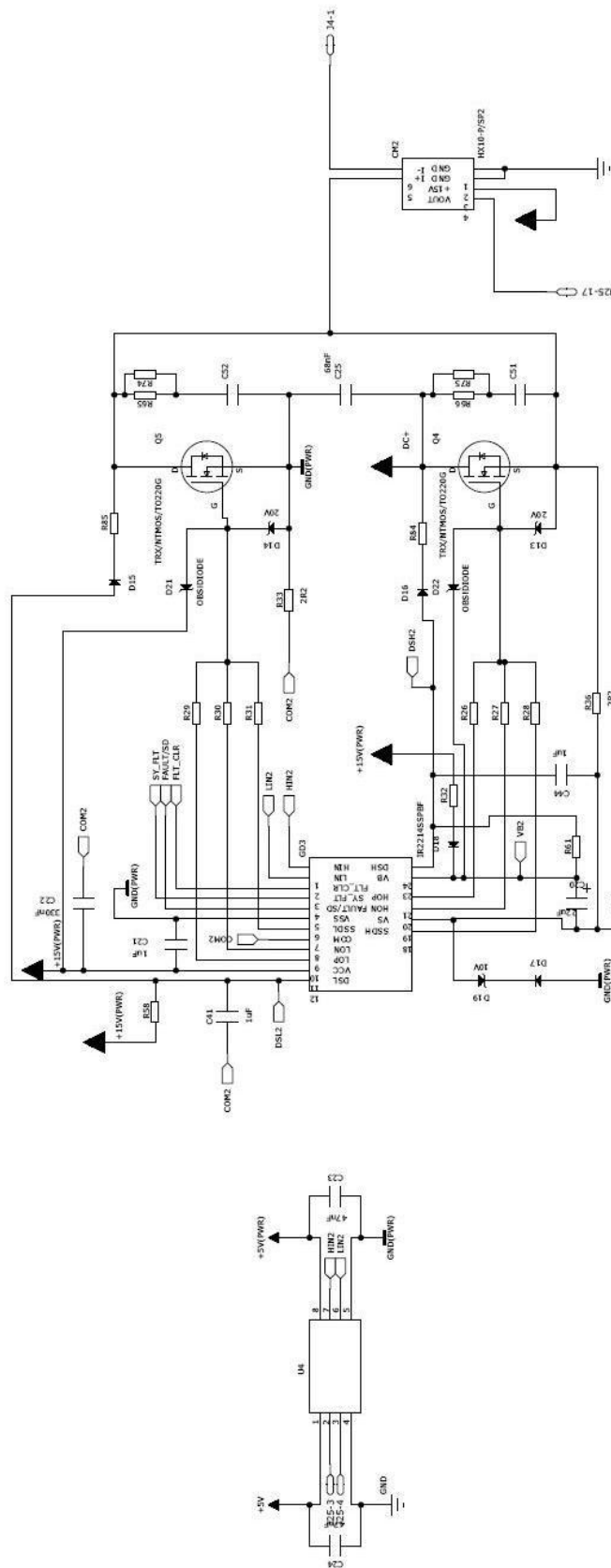
Figure 7-2 Schematics over the second inverter leg

Figure 7-3 Schematics over the third inverter leg

Figure 7-4 Schematics over the forth inverter leg

Figure 7-5 Schematics over the supply circuits